MONASH University

DYNAMICS PRECEDING ONSET AND TERMINATION OF ATRIAL FIBRILLATION AND VENTRICULAR TACHYCARDIA

A thesis submitted for the degree of Doctor of Philosophy

by

LIEW YEW WAI

Electrical and Computer Systems Engineering

Faculty of Engineering

Monash University

2019

COPYRIGHT NOTICE

ABSTRACT

Complex dynamical systems can shift abruptly from a stable state to an alternative stable state at a tipping point. Before the critical transition, the system either slows down in its recovery rate or flickers between the basins of attractions of the alternative stable states. However, whether the heart critically slows down or flickers before it transitions into and out of atrial fibrillation (AF) and ventricular tachycardia (VT), which are two common cardiac arrhythmias, is still an open question. In this thesis, we will address this fundamental question by studying the RR interval fluctuations derived from ECG data. We propose methods, which are currently non-existing, to define cardiac states based on the RR interval fluctuations, and to detect flickering. According to the theory of critical transition, an increasing lag-1 autocorrelation of the cardiac states is evidence for critical slowing down. On the other hand, flickering of the cardiac state between the two alternative basins of attractions would lead to a bimodal distribution of the cardiac states, where one mode corresponds to the Near-Normal State and the other mode corresponds to the Near-Disease State. Our results show flickering precedes the critical transitions for both AF and VT, instead of critical slowing down. Flickering of the cardiac state could be used as part of an early warning or screening system for the arrhythmias. It could also be used to develop new pharmaceuticals and control methods to prevent the onset of the arrhythmia, as well as new termination methods for intervention. Furthermore, the methods developed in this study may be adapted to study the dynamics preceding critical transition for other chronic episodic diseases.

DECLARATION

This thesis contains no material which has been accepted for the award of any other degree or diploma at any university or equivalent institution and that, to the best of my knowledge and belief, this thesis contains no material previously published or written by another person, except where due reference is made in the text of the thesis.

Signature:

Liew Yew Wai

March 2019

ACKNOWLEDGEMENTS

There are a number of people I would like to give my thanks and appreciation to, without whom this thesis would not have been completed. First and foremost I would like to thank my main supervisor, Dr. Lan Boon Leong for his guidance, dedication, the constructive criticisms, and most of all, for his patience. For all the lengthy discussions we have had to shape the direction and scope of this thesis. I hope to be able to say that I picked up a bit of his habit of utmost attention to details, and a little of his wisdom. To my co-supervisor, Dr. Liang Shiuan-Ni, thank you for the support and the encouragement throughout.

I would also like to thank the staff at Institut Jantung Negara. To Dr. Yap Lok Bin, for the initial meetings which paved the way and helped the project move forward. In particular, I would like to thank Dr. Suraya Hani, for her expertise and her time, busy as she was with her regular clinical schedules.

To the fellow postgraduates I have met, conversed with, and shared hopes (and sometimes frustrations!) throughout, thank you for making the course a lot less lonely. And finally to mom and dad, and to my brother. You've always been the rock of support that I fall back onto.

Liew Yew Wai

March 2019

TABLE OF CONTENTS

LIST OF FIGURES

LIST OF TABLES

CHAPTER 1

INTRODUCTION

1.1 Critical Transition

Complex systems refer to systems that have many interconnecting components that interact with each other, creating a large number of possible variables that are difficult to model thoroughly [2]. Dynamical systems describe systems that have phases or states that evolve or change over time [3]. Many complex dynamical systems from a wide range of fields exhibit tipping points where the system suddenly shifts from a stable state into a contrasting alternative stable state. This sudden shift from one stable state to an alternative stable state is known as a critical transition. Examples of critical transition include ecological systems [4-9], for example a forest or savannah area becoming barren, a sudden collapse of coastal ecosystems, arid ecosystems (lacking in rainfall) becoming deserts, and clear lakes becoming eutrophic (having excessive nutrients) leading to disruption of the aquatic life within the lake. The study of critical transition is also prevalent in efforts to understand changes to our earth's climate [10-12] and past global financial crises [13, 14]. In the fields of medicine and chronic diseases, examples of critical transition include asthma attacks [15], depression [16], diabetes [17, 18] epileptic seizures [19-21] and other conditions [22-25].

In critical transition theory, critical thresholds or tipping points correspond to catastrophic bifurcations in the system state [26, 27]. Figure 1 shows a model of critical transition with bifurcation i.e. tipping points at T_1 and T_2. The solid curve in the figure represent alternative stable states, which are also known as attractors [1]. The dotted curve represents unstable states, which is a border between the basins of attraction of the two alternative stable states. The basin of attraction of an attractor is the set of all initial states that ultimately converge to the attractor.

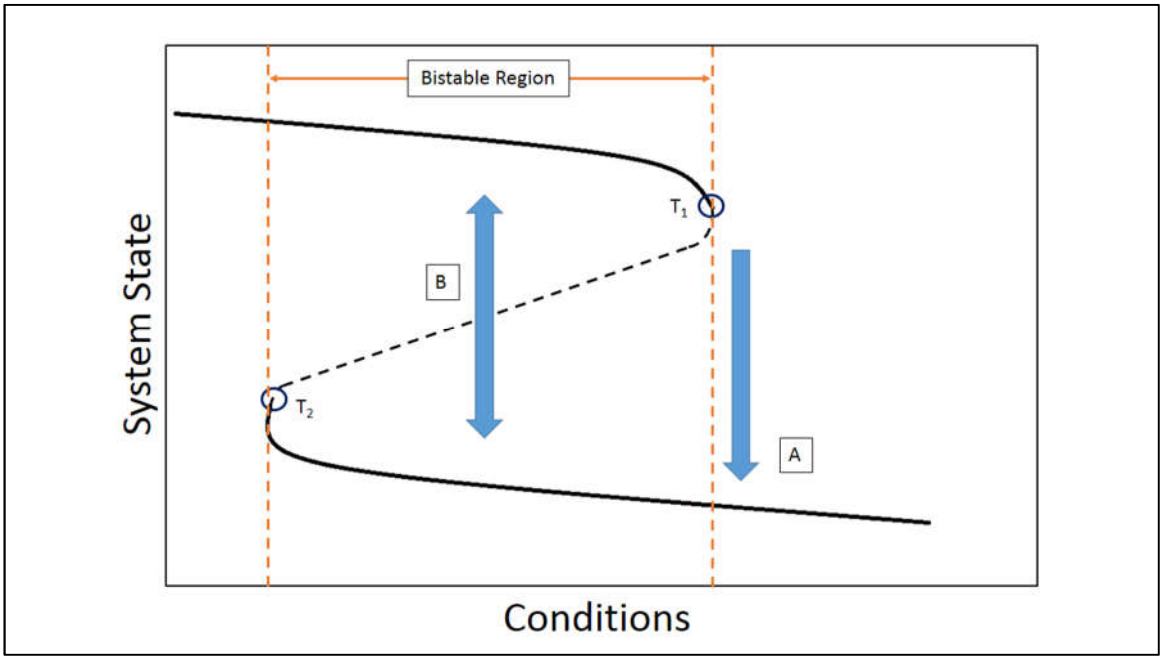

Figure 1. Model of critical transition. Figure adapted from [1]. The solid lines represent alternative stable states or attractors. The dashed line represents the border separating the two basins of attractions. Process [A] is a critical transition from one stable state to an alternative stable state at the bifurcation point T1. Process [B] is flickering between the basins of attraction of the two alternative attractors within the bistable region.

Critical transitions are hard to predict, as the system may show little change in state before the tipping point or critical threshold is reached [22, 27, 28]. However, there are certain signs common across many cases of critical transition as they approach the tipping point. Prior to the critical transition, systems can either experience 'critical slowing down', or 'flickering' [27, 28]. By identifying which of the mechanisms underlies the approach to the critical transition, the critical transition can be anticipated, and steps taken to avert the impending shift into a contrasting state.

Critical slowing down describes a known phenomenon in dynamical systems theory [29], whereby as a system approaches a tipping point it becomes increasingly slower in recovering from even small perturbations. Moreover, analysis of various models show that critical slowing down typically starts to occur even far from the bifurcation point (tipping point) and recovery rates decrease smoothly to zero as the tipping point is approached [30]. A simple dynamical model of critical slowing down, describing why recovery rates tend to zero when approaching the tipping point, was presented in Box 2 in [27]. The model has two equilibria, a stable state and the other is unstable (or an alternative stable state). It showed that when the state of the equilibrium is disturbed, the eigenvalue λ which represents the recovery rate of the system reaches zero at the bifurcation point where the two equilibria meet. The major implication from critical slowing down is that analysis of the recovery rates after a small experimental external perturbation can be used as an indicator of how close a system is to a tipping point, as the increased 'lethargy' of the system in recovering from perturbations can be detected in the form of a reduced rate of recovery [30, 31]. In addition to a reduced rate of recovery, critical slowing down also allows us to predict certain characteristic changes in the system, such as an increasing lag-1 autocorrelation of the fluctuations in the system state [28, 32]. The increasing pattern of the lag-1 autocorrelation can be easily understood: because critical slowing down causes the recovery rates to become increasingly slower near the tipping point, the current state of the system becomes increasingly similar to its recent past state between successive observations close to the tipping point [27].

Not all critical transitions are preceded by critical slowing down. In stochastic dynamical systems, a different phenomenon called flickering [27, 33] occurs near the bifurcation point. Flickering describes a behaviour whereby stochastic noise in the system moves the system

state back and forth across the boundary (dashed line in Figure 1) between the basins of attraction of two alternative stable states or attractors in the bistable region [34]. This would lead to a bimodal distribution of system states [28, 34, 35]. A stochastic model of flickering is the Threshold Autoregressive model. There are two stochastic processes in the model, where one process switches to the other at a threshold value. The two processes are described by two Autoregressive models – mathematical details of the model are given in [36]. In highly stochastic systems, flickering typically start to happen even when far away from bifurcation points [28], thereby making flickering behaviour also useful to be considered as an early warning to the proximity of a tipping point. Eventually, if the underlying change of conditions or perturbations to the system persists, the system shifts into the alternative stable state as a result of flickering. Flickering has been suggested to precede transitional shifts in ecological systems such as lake eutrophication and tropic cascades [37, 38], as well as characterising the end of the Younger Dryas cold climatic period leading into the current warmer Holocene epoch [12, 39].

1.2 Aims

In the context of diseases, we name the two alternative stable states or attractors as 'Normal State' and 'Disease State', and the corresponding basin of attraction as 'Near-Normal State' and 'Near-Disease State'. Olde Rikkert et al. [23] hypothesized recently that critical transition to the Disease State in chronic episodic disorders – such as asthma, cardiac arrhythmias, migraine, epilepsy and depression – are preceded by critical slowing down instead of flickering.

Only a couple of studies have addressed this hypothesis so far – a study on depression [16] and a study on epileptic seizure [40], which support the hypothesis. Thus, whether the hypothesis is true for other chronic episodic disorders is still an open question. The primary aim of this study is to investigate the hypothesis by focusing on two common cardiac arrhythmias, namely (i) Atrial Fibrillation (AF), and (ii) Ventricular Tachycardia (VT). Additionally, we will study if the hypothesis is true for the reverse transition, i.e. transition to the Normal State, for AF and VT.

For cardiac arrhythmias, earlier studies on the dynamics of the transition from normal sinus rhythm to arrhythmia are based only on theories of non-linear dynamics and chaos [41-45], which suggest that cardiac fibrillation is a form of spatial-temporal chaos that arises via a quasiperiodic transition [46, 47]. The emergence of cardiac arrhythmia has also been linked to a period-doubling bifurcation, which manifests as an alternating cardiac rhythm [48, 49].

For each of the chronic diseases, the dynamics preceding critical transition to arrhythmia will be studied through the analysis of RR interval fluctuations, which are obtained from electrocardiogram (ECG) data, during the Normal Sinus Rhythm (NSR) stage prior to the shift. The reverse transition from arrhythmia to NSR will be studied in the same manner. In the next chapter we will propose methods, which do not currently exist, to define cardiac states based on the RR interval fluctuations and to detect flickering.

It can be shown mathematically [27] that critical slowing down will lead to an increase in the lag-1 autocorrelation of the cardiac states. Other trends in the lag-1 autocorrelation function would rule out critical slowing down as the underlying mechanism. For flickering, there is no unique trend for the lag-1 autocorrelation, it could be either increasing [36] or

decreasing [34]. However, flickering between the Near-Normal and Near-Disease States would lead to a bimodal distribution [28, 35] of the cardiac states, where one mode corresponds to the Near-Normal State and the other mode corresponds to the Near-Disease State.

Before proceeding to the next chapter, some relevant background information will be given in the rest of this chapter. This includes information on cardiac beats and rhythms, as well as some information on the cardiac arrhythmias and their clinical classifications.

1.3 Cardiac Beats and Rhythms

In heart rate variability (HRV) analysis, there are many HRV metrics that have been suggested and used. These can be broadly grouped into 3 types, time-based measurements, frequency-based measurements, and non-linear measurements [50, 51]. Typically, the usual starting point of any HRV analysis is the RR interval. The RR interval refers to the time interval between two R-peaks of an ECG heart beat waveform – the 'R' notation is taken from the PQRST heart wave-complex. Occasionally, the notation 'NN' is used to indicate that only normal R-peaks are used in the analysis [52].

For the majority of healthy populations without any cardiac problems, the cardiac rhythm mainly consists of Normal Sinus Rhythm (NSR), typically described as a steady heart beating at a regular pace of between 60 to 100 beats per minute (bpm) [53]. There are some rare exceptions to this case, for example very fit athletes could have a heart rate as low as 40 bpm [54]. Irregularities of the cardiac heart rhythm (which affects the consistency of the

RR beat interval) can mainly be attributed to two causes – ectopic beats/rhythm and arrhythmia.

Ectopic beats are premature atrial or ventricular contractions of the heart. They are sometimes detected as singular, isolated premature beats but could also manifest in specific patterns and form an ectopic rhythm; among the common ectopic rhythms are *bigeminy* (one normal sinus beat alternated by one premature beat) and *trigeminy* (a repeated pattern of two normal sinus beats followed by one premature beat). A very high rate of detected ectopic beats could be of clinical significance of an underlying undetected heart disease [55] but most of the time, ectopic beats are benign and occasionally can occur even in healthy populations. Usually, no cause can be attributed to these occasional benign ectopic beats and they typically tend to disappear on their own after some time [56].

Arrhythmia generally describes a problem with the rate or rhythm of the heartbeat, which can be either too fast, too slow or highly irregular relative to what is considered healthy normal sinus rhythm. There are many types of arrhythmia, too numerous to sufficiently cover in this short introductory section, so I will only mention the arrhythmias relevant to our study – Atrial Fibrillation and Ventricular Tachycardia.

1.4 Cardiac Arrhythmias and Classifications

1.4.1 Atrial Fibrillation (AF)

Atrial fibrillation is one of the most common types of arrhythmia [57]. Patients with AF commonly experience an irregular heart rhythm coupled with tachycardia (very fast heart

rate), upwards of 400 bpm in some cases. AF can be classified according to the duration (and severity) of its episodes – *Paroxysmal* (episodes tend to terminate spontaneously on their own, usually within a week), *Sustained* or *Persistent* (requiring electrical or pharmacological cardioversion for termination), and *Permanent* (unable to be terminated even with intervening cardioversion) [58]. During episodes of AF, the upper and lower heart chambers become unsynchronised, and the lower chambers cannot function at full capacity to pump enough blood to the lungs and the rest of the body, causing patients to feel uncomfortable (from the irregular rhythm), tired, and dizzy [57]. A higher incidence of stroke has been associated with patients with untreated paroxysmal AF [59]. For some patients, AF can be an ongoing heart problem that lasts for years; eventually the symptoms can increase in duration and severity, which may lead to further serious complications.

1.4.2 Ventricular Tachycardia (VT)

In ventricular tachycardia, the cardiac dysfunction originates from the lower chambers of the heart (in contrast with AF which starts from the upper chambers). The electrical signals from the heart's lower chambers activate abnormally, interfering with the natural pacemaker operation of the heart [53]. As a result the heart chambers do not fill completely in between contractions, and blood flow to the rest of the body is compromised. Patients with VT experience a fast heart rate, often between 100-250 bpm with other symptoms associated with compromised blood circulation – dizziness, palpitations and even loss of consciousness. Prolonged episodes of VT (even more than a few seconds) can be very dangerous and intervention is recommended. Untreated, VT may degenerate into very serious conditions including ventricular fibrillation (VFib, disorganised electrical heart signals which leads to cardiac arrest), asystole (cardiac flatline) and sudden cardiac death

[59]. Classifications of VT typically include the duration of its episodes – *Paroxysmal* or *Non-Sustained VT* (asymptomatic, lasting for less than 30 seconds) and *Sustained VT* (VT that lasts for more than 30 seconds, or is symptomatic) [60] as well as some less clinically common classifications including *Persistent VT* (multiple recurrent Sustained VT) [61], and *Incessant VT* (continuous Sustained VT that can last for several hours, promptly reoccurring despite repeated intervention) [62]. Aside from duration characteristics, VT is also commonly described in terms of its QRS morphology (e.g. monomorphic or polymorphic).

CHAPTER 2

METHODOLOGY

Overview

In this chapter, we define cardiac states and propose how flickering prior to a critical transition can be detected.

2.1 Definition of Cardiac State

For this study, we adapted the usage of RR interval fluctuations (RRI fluctuations), defined as the difference between successive natural logarithm of the RR interval, from the work by Lan and Toda [63] to define cardiac state. Mathematically, the RRI fluctuations are given by

$$\mathbf{ln(RRI_i) - ln(RRI_{i-1})},$$

where RRI_i indicates the *i*th RR interval. This is similar to log-returns in the field of finance or econophysics [64], which is used to track the variability of the returns of investment over a specified time. The RRI fluctuation similarly measures the variability of the RRI intervals. The reason for using 'log-returns' rather than the non-transformed original data is because studying the changes can yield better insight of the underlying dynamics. The series of RRI fluctuations is divided into equal, non-overlapping data intervals (note that this is not the same as equal time-length windows). Each window has the same number of RRI fluctuations, but the total accumulated time within each separate window will be different due to natural variations in the RR intervals. Regardless, as our intent is to track the change from one window to the next subsequent window in the RRI fluctuation series, both equal data-length and equal time-length approach would work, but the equal data-length approach

was relatively easier to implement. The cardiac state in a window is defined by the standard deviation of the RRI fluctuations.

2.2 Normal and Disease States

To determine the distribution of standard deviations of the RRI fluctuations for the Normal State, we use the long term, sustained normal sinus rhythm (NSR) data from the MIT-BIH Normal Sinus Rhythm (MIT-BIH NSR) database [65]. For each dataset, after pre-processing (details in section 3.2) the RR intervals are calculated, followed by the RRI fluctuations. The RRI fluctuation series is then divided into non-overlapping, equal data-length windows. For each window, we calculate the standard deviation of the RRI fluctuations. The standard deviations obtained from all the datasets are used to determine the distribution.

For AF State (the corresponding Disease State in AF), sustained AF rhythm data was obtained from the Long Term Atrial Fibrillation database [66, 67]. The criteria for sustained AF rhythm samples was that the AF rhythm spanned the entire length of recorded data (each sample duration was between 20 – 24 hours). The distribution of standard deviations of the RRI fluctuations for the AF State is determined using the Sustained AF rhythm data in a similar manner as for the Normal State. The range of standard deviation of RRI fluctuations for the Normal State and AF State are shown in Figure 2.

For all data window sizes, the standard deviations of the RRI fluctuations for the Normal State and AF State are not normally distributed (D'Agostino–Pearson, p-value <0.001). The Mann-Whitney test showed significant difference between the standard deviations for the

Normal State and AF State (p-value <0.001). There is an overlap between the tail of the distribution of the standard deviations for the Normal State and AF State – see Figure 3, where the tails of the distributions intersect at about 0.125.

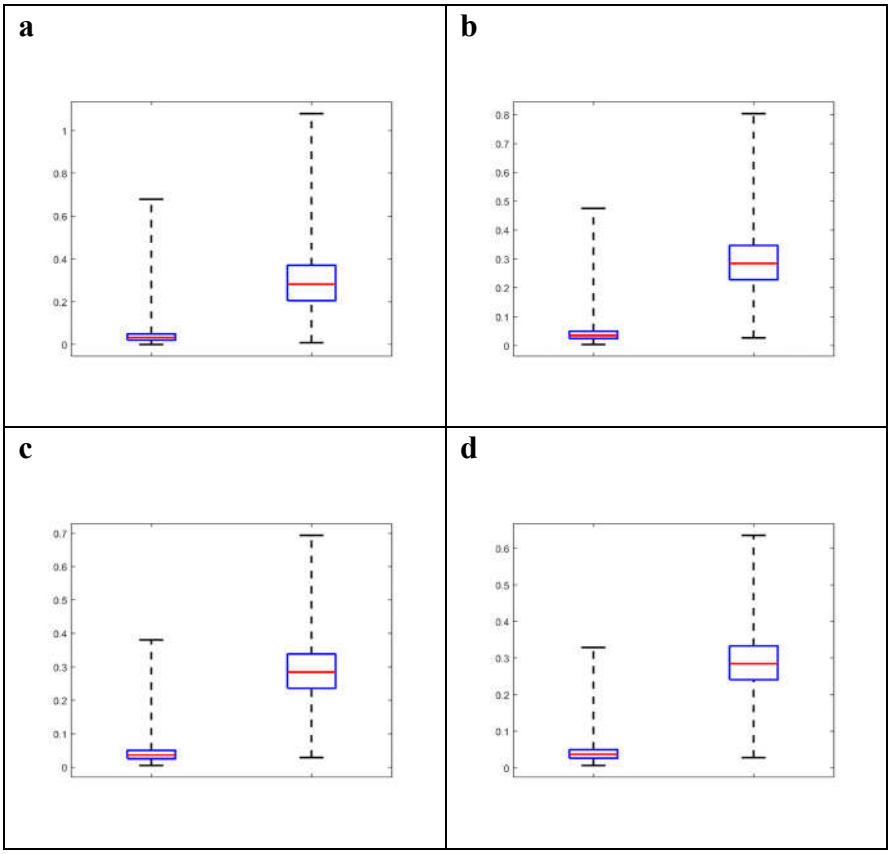

Figure 2. Range of standard deviations of RRI fluctuations for the Normal State (left) and AF State (right), for data window sizes of (a) 5, (b) 10, (c) 15 and (d) 20. Whiskers show minimum and maximum values.

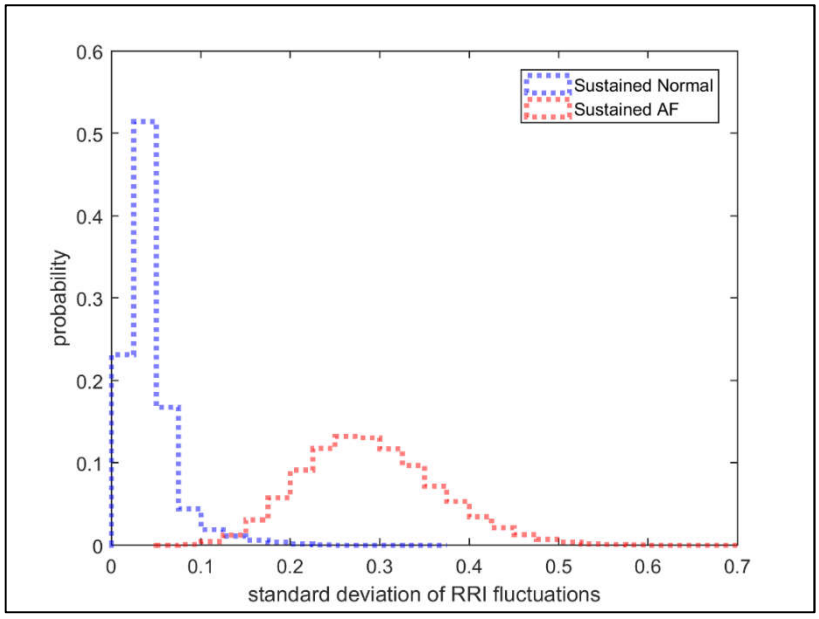

Figure 3. Distribution of standard deviations of RRI fluctuations, Normal State versus AF State, for window size 15.

For VT however, long term sustained cardiac rhythm data for these diseases are much harder to come by because in most cases during an opportune data recording when the disease manifests, intervention would have been applied by the monitoring clinical staff. Unlike sustained AF cardiac rhythm, which can be moderately tolerated without the risk of immediate life-threatening danger [68], sustained VT rhythm can lead to ventricular fibrillation which is life threatening [59]. The classification of VT rhythm that would be most suitable for use to define VT State (i.e. the Disease State for VT) is the rare form known as Incessant VT. We were unable to obtain data for Incessant VT.

2.3 Near-Normal and Near-Disease States, and Flickering Detection

For the data segment before AF onset or termination, if the distribution of the standard deviations of RRI fluctuations is bimodal, where one mode is close to the Normal State

distribution (low standard deviations) and the other mode is close to the AF State distribution (high standard deviations), the standard deviations in the former and latter modes can be attributed to respectively Near-Normal and Near-AF States. The cardiac state flickers between the Near-Normal State and Near-AF State if the standard deviation switches between the low and high values repeatedly.

For VT, although we lack data for Incessant VT to define the VT State, the Normal State distribution is sufficient as a reference for comparison. For a pre-transition segment, if the distribution of the standard deviations of RRI fluctuations is bimodal, the standard deviations in the mode that is close to the Normal State distribution can be attributed to Near-Normal State, whereas the standard deviations in the mode that is not close to the Normal State distribution can be attributed to Near-VT State. Flickering of the cardiac state is evidenced if the standard deviation switches between values in the former and latter modes.

CHAPTER 3

DATASETS

3.1 Source and Selection

All data in this study was obtained from Physionet [69, 70], a large collection of high-quality physiologic signals made publicly available under the ODC Public Domain Dedication and License. The following subsections detail information regarding each of the databases sampled from, and the sampling criteria.

ECG-based datasets in the Physionet repository typically include the original (digitised) ECG waveforms, corresponding R-peak timings as well as additional information in the form of beat and rhythm annotations contributed by various researchers who collected the original data. In the context of digitised ECG data, a 'beat' refers to an R-peak and its timing information (counted from start of data record, and/or the time interval from the last detected beat). The R-peaks are usually detected, and compiled using an R-peak detection algorithm scanning through the digitised ECG waveform. Beat annotations give information for every individual beat, whether it is normal or ectopic, but can also contain more advanced information such as an expected, but missing beat (predicted based on moving pattern of previous beats), or a noise distortion which could mask a genuine beat. Rhythm annotations – typically tagged onto the closest beat prior to a change in cardiac rhythm – mark the start of a rhythm section (and the end of the previous rhythm). Noise artifacts can be presented as either beat, or rhythm annotations.

All databases available on Physionet are anonymised. Some non-identifiable information are sometimes included (e.g. age, gender and medication if relevant). Often the samples in the database can be multiple sets of records from the same patients, or some of the data

collected during the original study has been excluded from the database because of confounding factors.

3.1.1 Sustained Normal Sinus Rhythm Data

Data for long term, sustained normal sinus rhythm (NSR) is obtained from the MIT-BIH Normal Sinus Rhythm Database (MIT-BIH NSR) (Table 1). There are 18 datasets in this database, each about 24 hours in duration collected from subjects who were verified to have had no arrhythmias. The subjects include 5 men aged between 26 – 45 years, and 13 women aged between 20 – 50 years [65, 69]. The majority of the beats are annotated as normal, and a non-significant number of beats are ectopic (0.02%), which is common in a healthy heart [56]. Noise is indicated as beat annotations. All 18 datasets in the MIT-BIH NSR Database were used to compile reference standard deviations of RRI fluctuations for Normal State.

Table 1. Sustained normal sinus rhythm samples from MIT-BIH NSR database.

No.	Physionet Record	Length (hours)	Length (data points)
1	nsr16265.atr	25.4	99408
2	nsr16272.atr	25.0	83448
3	nsr16273.atr	24.6	89389
4	nsr16420.atr	23.9	101432
5	nsr16483.atr	25.9	103925
6	nsr16539.atr	24.6	107548
7	nsr16773.atr	23.9	47208
8	nsr16786.atr	24.5	101425
9	nsr16795.atr	23.5	85520
10	nsr17052.atr	23.1	86602
11	nsr17453.atr	24.4	99720

12	nsr18177.atr	25.9	114561
13	nsr18184.atr	23.7	101822
14	nsr19088.atr	23.8	76475
15	nsr19090.atr	24.1	80855
16	nsr19093.atr	23.2	64747
17	nsr19140.atr	24.1	96320
18	nsr19830.atr	23.2	108041

3.1.2 Atrial Fibrillation (AF) Data

The Long-Term Atrial Fibrillation Database (LTAF) [66, 67, 69] consists of 84 records (each 20-24 hours) of subjects with paroxysmal or sustained AF (alongside various other types of arrhythmia). Both beat and rhythm annotations are available, via a manual review of the output of an automated ECG analysis system courtesy of MEDICALgorithmics Ltd (Warsaw, Poland).

The LTAF database originated from a study by Petrutiu et.al [67], who studied spontaneous termination of paroxysmal atrial fibrillation (PAF). Additional information regarding the subjects in the study can be found from this excerpt from the paper, "A total of 44 patients were included in this study, 24 with PAF and a control group of 20 patients with sustained AF. Patients with PAF ranged from 43 to 89 years (mean ± SD, 67 ± 11 years). There were 12 men and 12 women. Patients with sustained AF ranged in age from 39 to 87 years (66 ± 12 years). There were 15 men and 5 women. Twenty-six patients were not taking any cardioactive drugs. Eighteen patients were taking cardioactive medications including beta-blockers (10 patients), calcium channel blockers (6 patients), digoxin (1 patient) and amiodorone (1 patient)" [67].

The LTAF database included 12 datasets where the sustained AF rhythm spanned the entire length of the data (around 24 hours each) without self-terminating into NSR or transposing into a different cardiac arrhythmia. These 12 datasets were used to compile reference values for AF State (Table 2) using the methodology outlined in the previous chapter.

For paroxysmal AF onset and termination, the following sample selection criteria (below) was used. For uniformity a similar sample selection criteria is used for both onset and termination.

AF Onset Sample Selection Criteria:

- Each sample consists of a pair of consecutive rhythms, specifically NSR rhythm transitioning into AF rhythm.
- The first and last set of rhythms in each dataset is excluded from selection, to remove the possibility of truncated data i.e. all rhythm selected are complete in terms of actual start, and endpoint of the rhythm.
- Duration criteria – For pre-transition NSR rhythm ("Pre-AF"), 5 samples were selected from each category - '15-30 minutes', '30 minutes–1 hour', '1–2 hours' and 'above 2 hours' - to adequately represent the duration ranges available. No duration criteria was imposed on the following AF rhythm.

AF Termination Sample Selection Criteria:

- Each sample consists of a pair of consecutive rhythms, specifically AF rhythm transitioning into NSR rhythm.

- The first and last set of rhythms in each dataset is excluded from selection, to remove the possibility of truncated data, i.e. all rhythm selected are complete in terms of actual start, and endpoint of the rhythm.
- Duration criteria – For AF rhythm, 5 samples were selected from each category - '15-30 minutes', '30 minutes–1 hour', '1–2 hours' and 'above 2 hours' - to adequately represent the duration ranges available. No duration criteria was imposed on the following NSR rhythm.

In total, the number of data samples collected for the AF study was 12 for the reference AF State, 20 for the AF onset subset (Table 3) and 20 for the AF termination subset (Table 4).

Table 2. Sustained AF rhythm samples from LTAF database.

No.	Physionet Record	Length (hours)	Length (data points)
1	12.atr	24.1	117141
2	17.atr	24.8	138057
3	18.atr	24.9	141510
4	21.atr	20.9	81590
5	54.atr	24.9	118196
6	69.atr	23.7	141521
7	70.atr	26.1	128333
8	71.atr	24.0	125199
9	75.atr	20.8	126769
10	202.atr	23.9	145621
11	205.atr	23.8	116498
12	208.atr	23.9	120740

Table 3. AF onset samples from LTAF database.

No.	Physionet record	Start Sample #	End Sample #	Length (minutes)	Length (data points)
1	16.atr	7814978	8008281	25.2	2024
2	28.atr	6137071	6267517	16.9	1057
3	39.atr	908273	1086583	23.2	2024
4	55.atr	8501531	8667459	21.6	1431
5	104.atr	2938232	3078843	18.3	1654
6	06.atr	1462835	1712593	32.5	2444
7	08.atr	1193512	1454383	33.9	2406
8	16.atr	8914669	9181420	34.7	2826
9	45.atr	8235043	8631336	51.6	2964
10	104.atr	251969	573629	41.8	3578
11	05.atr	6142734	6614565	61.4	4938
12	51.atr	4919271	5538182	80.6	5328
13	110.atr	803255	1683075	114.5	9173
14	115.atr	171497	728545	72.5	5746
15	116.atr	2801091	3335027	69.5	6145
16	08.atr	4152729	10197279	787.1	58798
17	35.atr	936004	3022380	271.6	17231
18	102.atr	3518805	6510073	389.5	25487
19	104.atr	784823	1945472	151.1	12945
20	116.atr	4278071	5240930	125.3	9403

Table 4. AF termination samples from LTAF database.

No.	Physionet Record	Start Sample #	End Sample #	Length (minutes)	Length (data points)
1	03.atr	8220287	8361252	18.3	1475
2	06.atr	84888	271318	24.3	2870
3	28.atr	6653733	6774889	15.8	2064
4	42.atr	1968181	2192454	29.2	3461
5	105.atr	9345883	9504247	20.6	1151

6	03.atr	8364287	8657694	38.2	3588
7	39.atr	3575542	3808159	30.2	3057
8	51.atr	4248960	4682899	56.5	3719
9	200.atr	1934327	2331593	51.7	3214
10	200.atr	10100154	10436367	43.7	2235
11	35.atr	4832998	5593149	99.0	7026
12	39.atr	2882805	3406245	68.1	6854
13	39.atr	3928464	4394407	60.6	5587
14	72.atr	9225225	9871750	84.1	8379
15	121.atr	6085527	6933986	110.4	10312
16	07.atr	8510411	9447553	122.0	10988
17	56.atr	5235075	9279261	526.5	46165
18	105.atr	7242184	8823033	205.8	9805
19	117.atr	319311	4052981	486.1	62395
20	122.atr	3692357	6428070	356.2	19083

3.1.3 Ventricular Tachycardia (VT) Data

Data for VT samples are obtained from the LTAF database described above in addition to 2 other separate databases listed here. The MIT-BIH Arrhythmia Database (MITDB) was originally compiled as standard test material for evaluation of cardiac arrhythmia detector performance (dating back to 1980), and later expanded its usage into research for cardiac dynamics [69, 71, 72]. The database contains 48 records, each approximately 30 minutes in duration. The source of the recordings is a set of long-term Holter recordings obtained by the Beth Israel Hospital Arrhythmia Laboratory (now the Beth Israel Deaconess Medical Center (BIDMC), Boston, USA). Subjects were sampled from a mixture of inpatients and outpatients to the hospital at 60:40 ratio. The subjects were 25 men (age 32 to 89 years) and 22 women (age 23 to 89 years) [73].

Approximately half of the records (23 out of 48) in the MITDB were selected at random from the original Holter set, and the remaining were chosen to include a variety of rare but clinically important cardiac arrhythmia samples that otherwise would not be well represented by small random sampling. In the first batch of 23, the random sampling was performed by using a random number table to select Holter tapes, and then to select half-hour segments from each, which finally passed a signal quality check by experts. The second batch of records were selectively chosen to include rare and complex arrhythmias and cardiac abnormalities, as well as for features of rhythm, QRS morphology variation, or signal quality which might be expected to present difficulties for arrhythmia detectors [73]. The types of arrhythmias in this database include (but not limited to) ectopic rhythms, supraventricular tachyarrhythmia, both atrial and ventricular flutter, as well as paroxysmal AF and VT.

Both beat and rhythm annotations are included with the MITDB database. The initial beat detection and annotation was performed by a simple QRS detector, which labelled each beat as a normal beat. This was later independently edited by two cardiologists, who added missing and/or deleted erroneous beat placements, changed labels to correctly identify abnormal beats, as well as adding in rhythm annotations, signal quality labels and other additional comments. Any discrepancies between the two independent cardiologists were resolved by consensus.

The other source of VT samples came from the MIT-BIH Malignant Ventricular Arrhythmia Database (VFDB), which consists of 22 recordings, each approximately 30 minutes long in duration, of subjects who experienced episodes of sustained VT, ventricular flutter (VFlutter), or ventricular fibrillation (VFib) [69, 74, 75]. There were no beat

annotations included with the VFDB database, although rhythm annotations were available. To obtain the R-beat timings, we used a commercial heart rate variability analysis software which also included an R-peak detection algorithm. After obtaining the R-peak timings, the RR intervals and RRI fluctuations can be calculated.

The recordings in the VFDB database originate from a research masters study to develop arrhythmia detection schemes to discriminate VT, VFlutter and VFib from electrode motion noise [75]. The original database was compiled, specifically, to include examples of ventricular arrhythmias (a general term inclusive of VT, VFlutter and VFib) and a secondary database containing electrode motion artifacts. Long-term Holter recordings from 16 patients (age and gender not disclosed) with ventricular arrhythmias were obtained from ECG tape libraries of Brigham and Women's Hospital (Boston, USA) and the Beth Israel Hospital (now Beth Israel Deaconess Medical Center, Boston, USA). 22 half-hour segments (those included in the VFDB database) from the long-term Holter records were digitised and selected as the ventricular arrhythmia dataset. Rhythm annotations were later manually added in, each change in rhythm is indicated by the starting time counted from the beginning of the sample.

For VT onset and termination, the sample selection criteria needed to take into account the relatively shorter duration of records in the two databases – both the MITDB and the VFDB database contained records of approximately 30 minutes in duration each – and the fact that paroxysmal VT generally only lasts for less than 1 minute [59] before self-terminating. A minimum duration for VT rhythm samples is however necessary to ensure there was enough data for meaningful analysis. The smaller pool of available VT rhythm data also meant that we could not afford to exclude the first and last set of rhythms from each data sample as we

did for AF, therefore there is a possibility that some of the rhythm data is truncated. This is particularly true for the MITDB database, since some of the records were originally compiled by random sampling of 30 minute duration blocks. Similar to paroxysmal AF, both onset and termination of VT samples were collected for analysis. The sample selection criteria for onset and termination of VT rhythm are outlined below, using the same criteria for LTAF, MITDB and VFDB databases.

VT Onset Sample Selection Criteria:

- Each sample consists of a pair of consecutive rhythms, specifically NSR rhythm transitioning into VT rhythm.
- Duration criteria – Pre-transition NSR rhythm ("Pre-VT") of minimum 5 minutes (300 seconds), followed by VT rhythm of any duration.

VT Termination Sample Selection Criteria:

- Each sample consists of a pair of consecutive rhythms, specifically VT rhythm self-terminating into NSR rhythm.
- Duration criteria – VT rhythm of minimum 30 seconds, followed by NSR rhythm of any duration.

Based on the sample selection criteria, there are 12 samples for VT onset (Table 5) and 3 samples for VT termination (Table 6).

Table 5. VT onset samples. Database sources: *LTAF, [+]MITDB and [#]VFDB.

No.	Physionet Record	Start Sample #	End Sample #	Length (minutes)	Length (data points)
1	47.atr*	4119703	4176961	7.4	725
2	47.atr*	5567829	5609895	5.4	363
3	56.atr*	9279328	9437410	20.5	2240
4	118.atr*	4274082	5529137	163.4	11897
5	205.atr[+]	229	107505	5.0	450
6	205.atr[+]	110298	333687	10.3	949
7	205.atr[+]	334395	525692	8.8	755
8	215.atr[+]	64973	443058	17.5	1961
9	223.atr[+]	49694	208009	7.3	617
10	420.atr[#]	69038	357538	19.2	1286
11	422.atr[#]	253961	333211	5.2	535
12	612.atr[#]	18	426846	28.4	1330

Table 6. VT termination samples. Database sources: [+]MITDB and [#]VFDB.

No.	Physionet Record	Start Sample #	End Sample #	Length (seconds)	Length (data points)
1	223.atr[+]	208252	227765	55.0	97
2	223.atr[+]	375669	389421	38.9	67
3	421.atr[#]	333961	371519	151.2	513

3.2 Data Pre-processing

A custom pre-processing filter was applied on all samples for AF and VT prior to analysis. It consisted of a 'non-physical' filter which checked and removed instances of RRI > 3 seconds. A concurrent filter checked for noise-annotated beats and removed affected RRI values. The filter was applied before calculating the RRI fluctuations. Noise-annotated

rhythms are avoided by specifying the rhythm types accepted in the sample selection criteria.

CHAPTER 4

RESULTS

Overview

The results of the study will be grouped and presented by disease type. For each of the diseases, first the lag-1 autocorrelation results will be presented and analysed. This will then be followed by the analysis for flickering preceding onset, and finally analysis for flickering preceding termination.

The lag-1 autocorrelation function is given by:

$$\boldsymbol{\rho_1 = \frac{E[(z_t - \mu)(z_{t+1} - \mu)]}{\sigma_z^2}},$$

where μ is the mean and σ^2 is the variance of variable z_t [76]. Input data for the lag-1 autocorrelation uses the standard deviation values of RRI fluctuations calculated in non-overlapping windows for various window sizes. The lag-1 autocorrelation is calculated in a moving window at 50% of input data length.

For AF, the standard deviations of RRI fluctuations are calculated in non-overlapping window sizes of 5 to 20 data points, in increments of 5. For VT, the window size is limited to only 5 and 10, due to the very short durations of the VT termination samples. All figures presented in this chapter are based on calculations using window size of 10.

4.1 AF Analysis and Results

4.1.1 Trend in Lag-1 Autocorrelation

Figures 4 and 5 show the lag-1 autocorrelation trends prior to AF onset and termination, respectively.

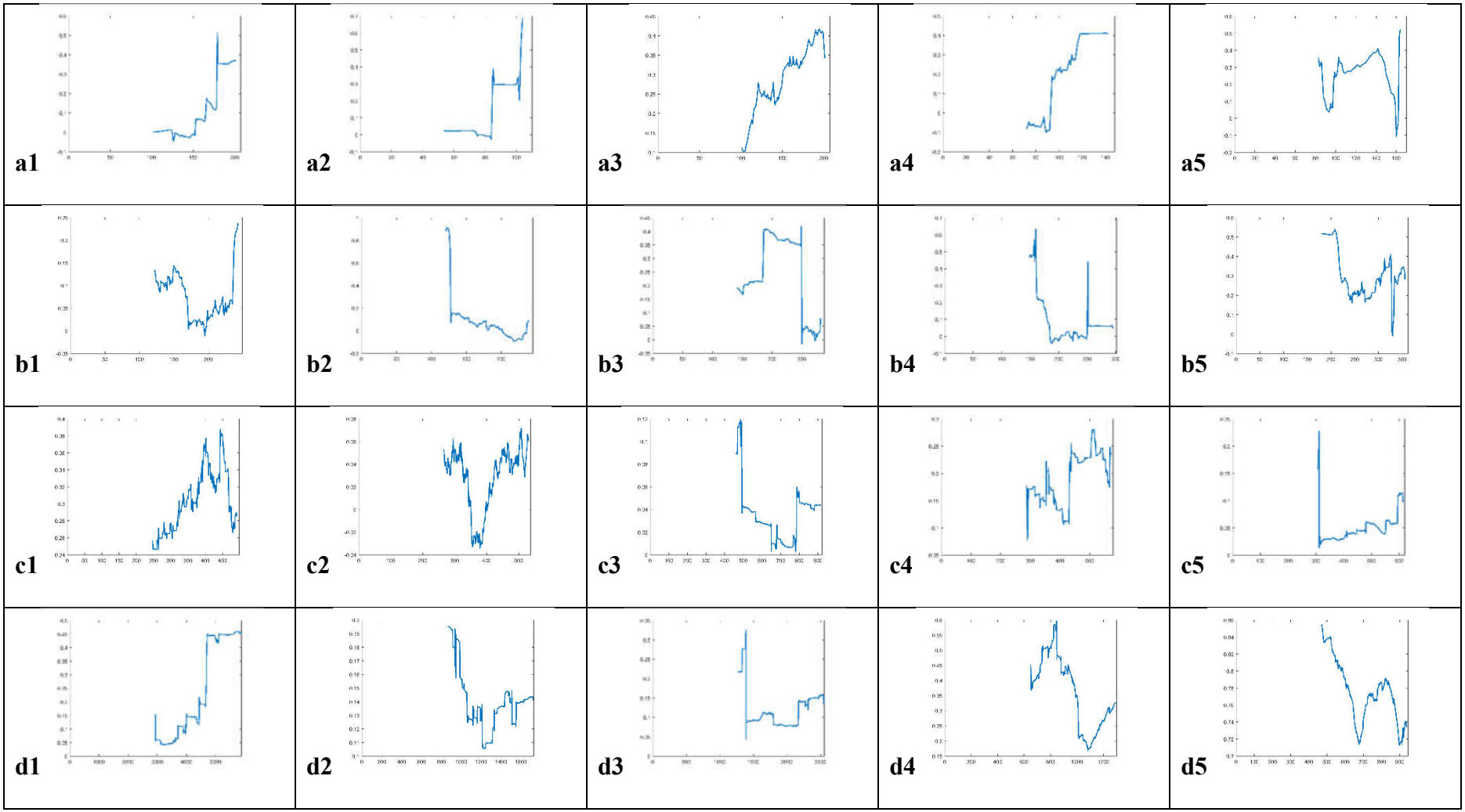

Figure 4. Lag-1 autocorrelation prior to AF onset. Y axis: Autocorrelation at lag-1, X axis: Data index at the end of the moving window used for the autocorrelation calculation. Pre-AF durations indicated by (t). (a1-a5) 15mins<t<30mins, (b1-b5) 30mins<t<1h, (c1-c5) 1h<t<2h and (d1-d5) t>2h. Sequence of samples follow the indexing order in Table 3 (a1=1, a2=2, etc.).

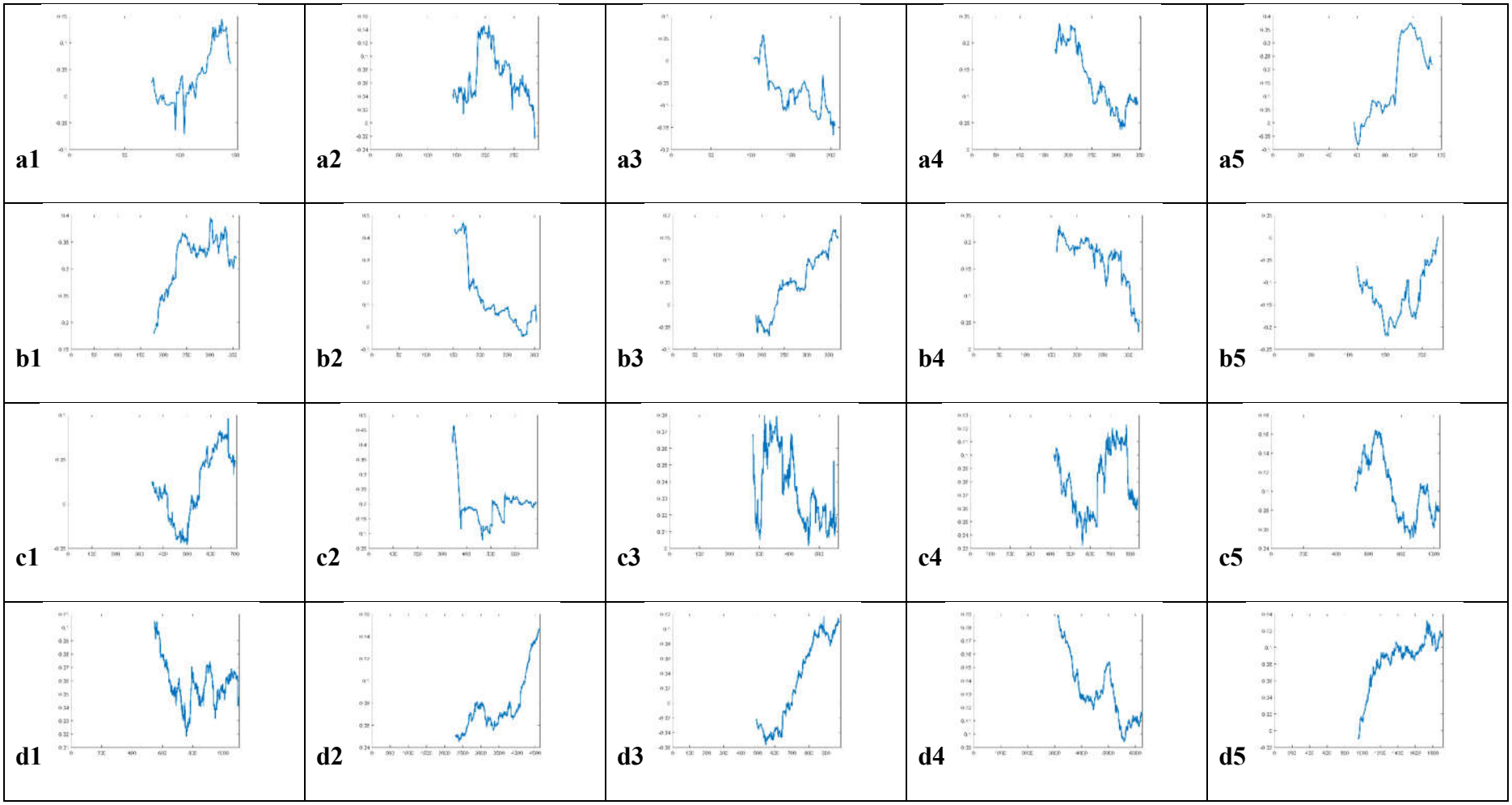

Figure 5. Lag-1 autocorrelation prior to AF termination. Y axis: Autocorrelation at lag-1, X axis: Data index at the end of the moving window used for the autocorrelation calculation. AF durations indicated by (t). (a1-a5) 15mins<t<30mins, (b1-b5) 30mins<t<1h, (c1-c5) 1h<t<2h and (d1-d5) t>2h. Sequence of samples follow the indexing order in Table 4 (a1=1, a2=2, etc.).

Critical slowing down will lead to an increase in the lag-1 autocorrelation of the cardiac states near the transition [28]. However here there is no indication of any common pattern among the results, with some of the lag-1 autocorrelation showing an increasing trend near the transition for AF onset (Figs 4a2, 4a5, 4b1, 4c5 and 4d3) as well as for AF termination (Figs 5b3, 5b5, 5d2, 5d3 and 5d5). Meanwhile other samples show a prominent decreasing lag-1 autocorrelation trend near onset (Figs 4b2, 4b3, 4c1 and 4d5), and similarly near termination (Figs 5a1, 5a2, 5a3, 5a5, 5b4, 5c4 and 5d4). In many samples for both onset and termination, it merely fluctuates without a clear trend (Figs 4a1, 4a3, 4a4, 4b4, 4b5, 4c2, 4c3, 4c4, 4d1, 4d2, 4d4, 5a4, 5b1, 5b2, 5c1, 5c2, 5c3, 5c5 and 5d1). The lag-1 autocorrelation results indicate that critical slowing down is not the underlying mechanism for the critical transition for either AF onset or termination. These results are similar for all window sizes of input data for the lag-1 autocorrelation.

4.1.2 Flickering Prior to AF Onset

The standard deviations of RRI fluctuations for each Pre-AF sample are significantly different from the values for the Normal State (Mann-Whitney test, p-value <0.001 for all). Thus the cardiac state is not Normal prior to AF onset.

Figure 6 shows the distribution of standard deviations of RRI fluctuations for a Pre-AF sample. Two modes are apparent in the distribution: one mode is close to the distribution for the Normal State and the other mode is close to the distribution for the AF State. Thus the standard deviations in the former and latter modes can be attributed to respectively Near-Normal and Near-AF States.

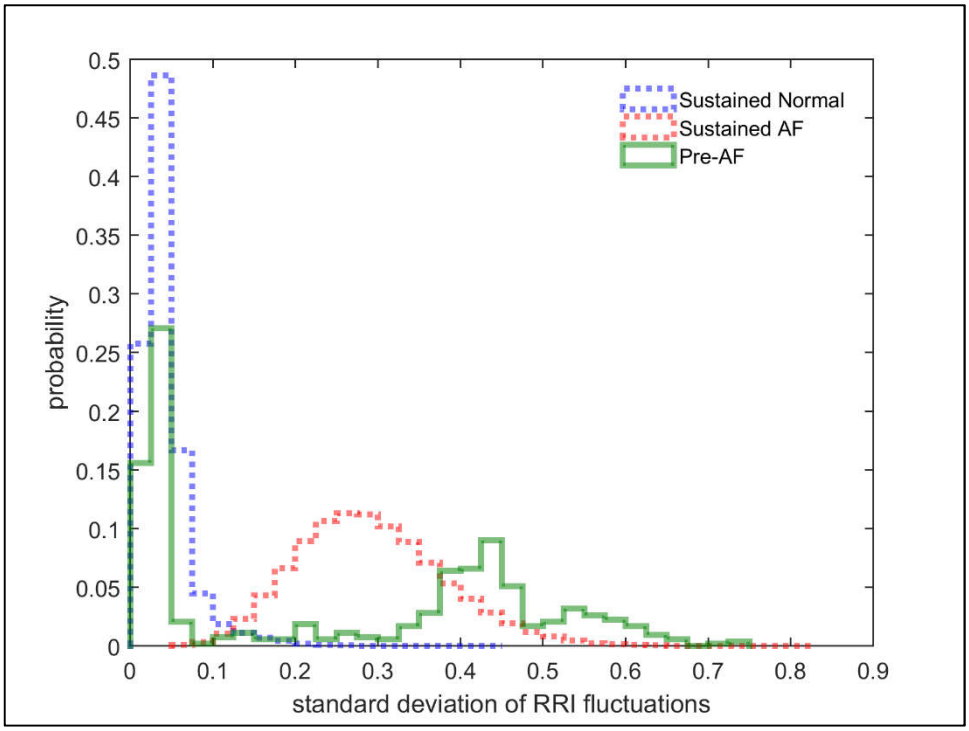

Figure 6. Distribution of standard deviations of RRI fluctuations for a Pre-AF sample, which is bimodal, superimposed on the distributions for the Normal State and AF State.

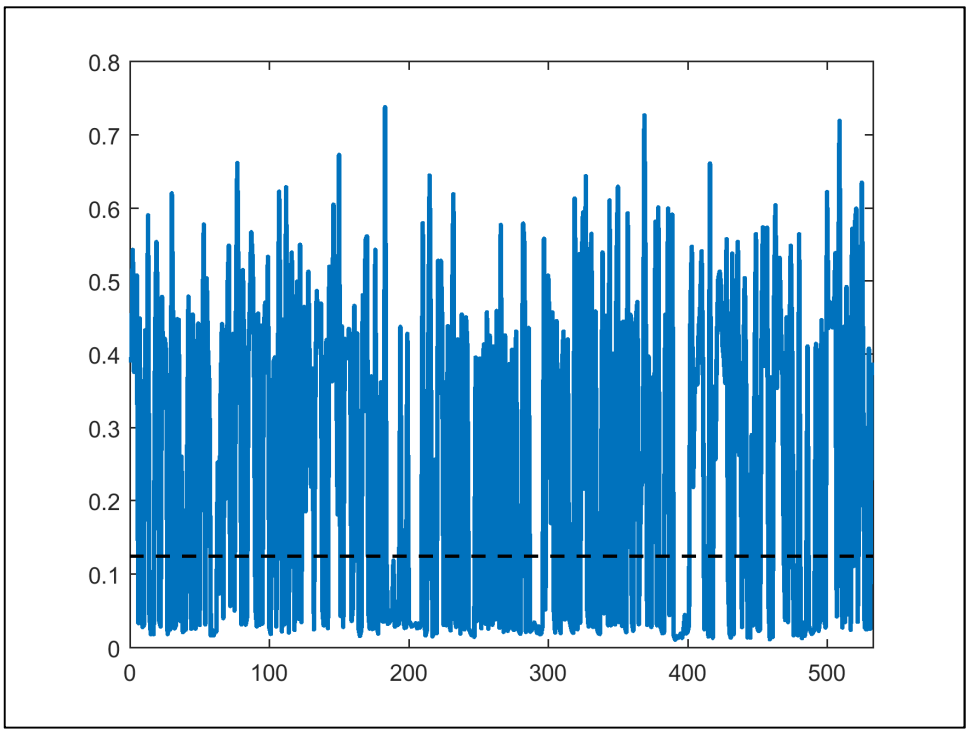

Figure 7. Time series of the standard deviation of RRI fluctuations for the Pre-AF sample in Figure 6. The horizontal dotted line is the boundary between Near-Normal and Near-AF.

From the histograms in Figure 6, the boundary between the Near-Normal and Near-AF standard-deviation values can be estimated to be where the distributions for the Normal and AF States intersect, which is approximately at 0.125. Based on this boundary, the standard deviation time series in Figure 7 shows that flickering between the Near-Normal and Near-AF States occurs very often throughout, up until the heart finally undergoes critical transition.

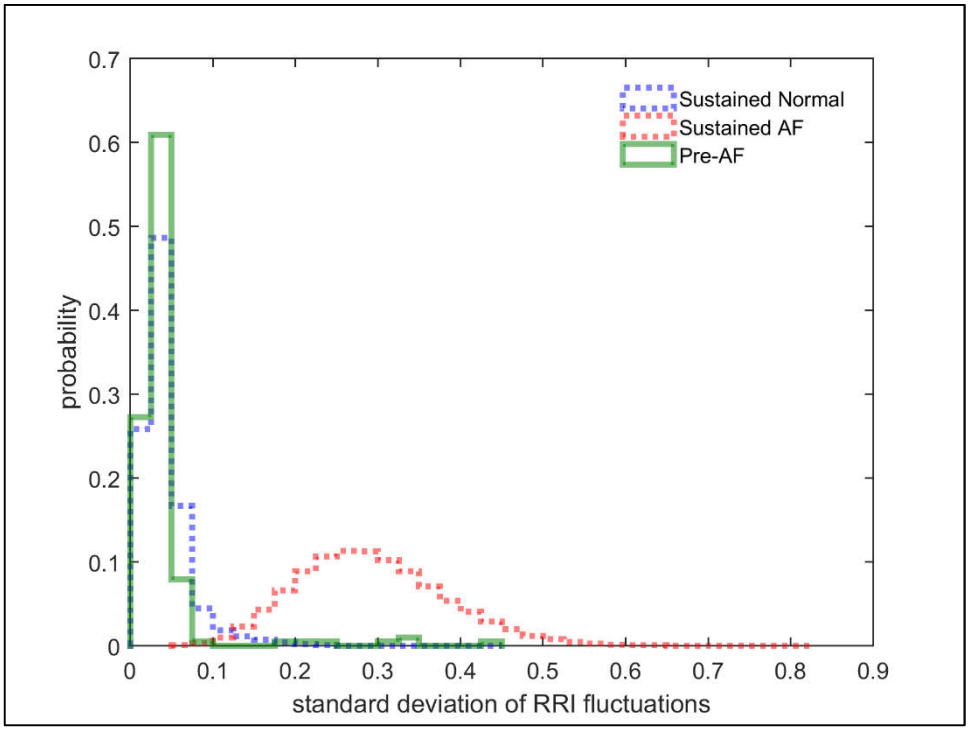

Figure 8. Distribution of standard deviations of RRI fluctuations for a Pre-AF sample, which is dominated by the Near-Normal mode, superimposed on the distributions for the Normal State and AF State.

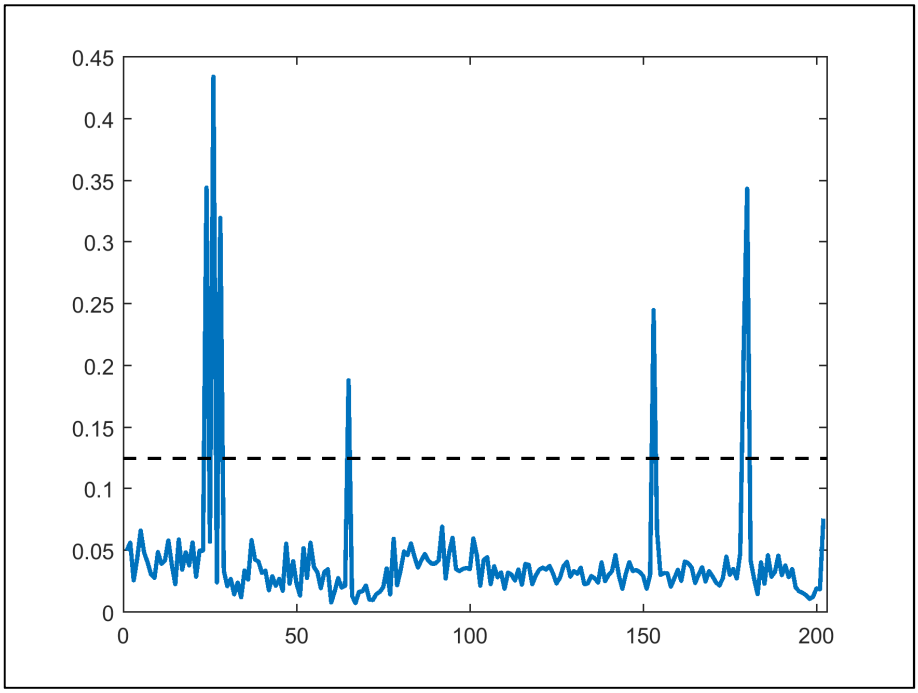

Figure 9. Time series of the standard deviation of RRI fluctuations for the Pre-AF sample in Figure 8. The horizontal dotted line is the boundary between Near-Normal and Near-AF.

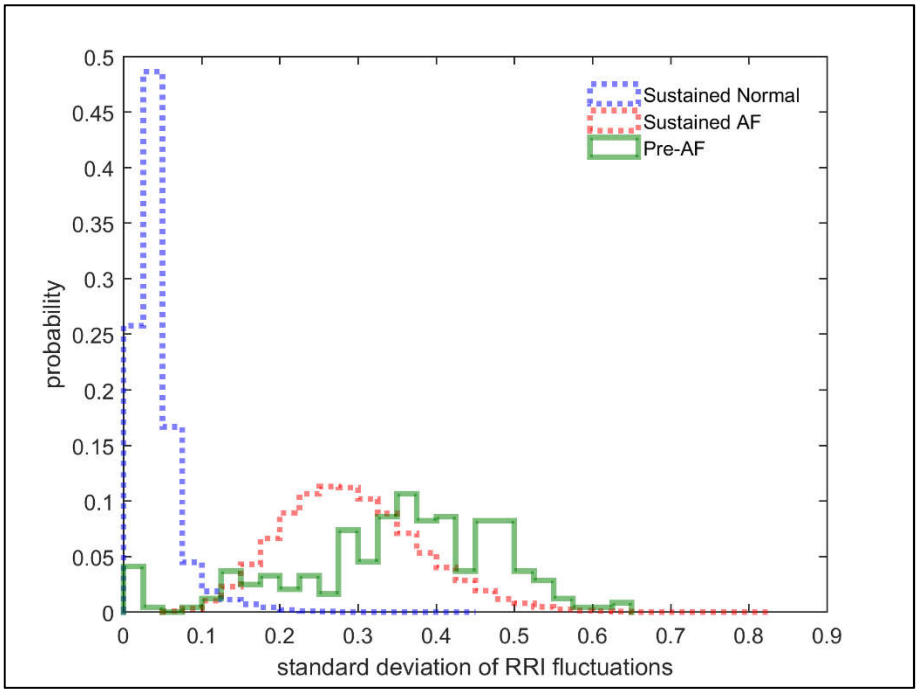

Figure 10. Distribution of standard deviations of RRI fluctuations for a Pre-AF sample, which is dominated by the Near-AF mode, superimposed on the distributions for the Normal State and AF State.

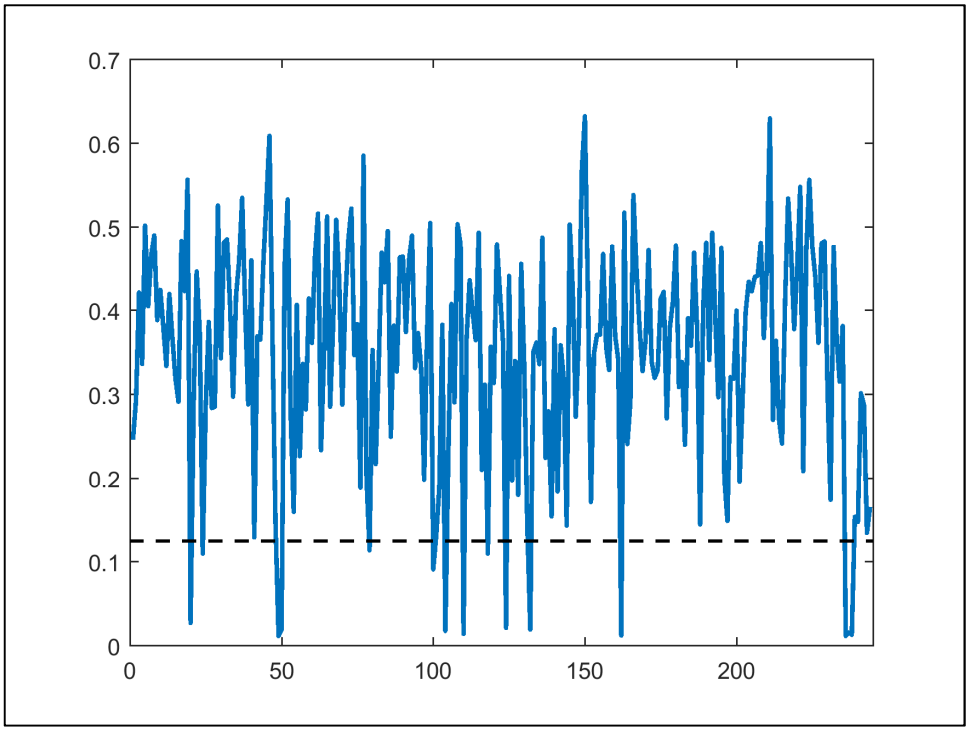

Figure 11. Time series of the standard deviation of RRI fluctuations for the Pre-AF sample in Figure 10. The horizontal dotted line is the boundary between Near-Normal and Near-AF.

A distinct bimodal distribution of standard deviations as the one shown in Figure 6 is apparent in 6 out of the 20 AF onset samples (dataset no. 4, 5, 10-12, and 20 in Table 3). The value of 0.125 is also a good approximation for the boundary between the Near-Normal and Near-AF standard-deviation values in these cases. Based on this boundary, the majority of the Pre-AF samples (12 of 20) have distributions which are dominated by the Near-Normal mode (dataset no. 1, 2, 7-9, 13-19 in Table 3), such as shown in Figure 8. The remaining 2 samples have distributions which are dominated by the Near-AF mode (dataset no. 3 and 6 in Table 3) - one example is shown in Figure 10. For these two types of distributions which are dominated by one mode, flickering still occurs. However, the cardiac state spends an inordinate amount of time either Near-Normal (Figure 9) in the

former case or Near-AF (Figure 11) in the latter case, while only occasionally flickering over to the alternative basin of attraction.

4.1.3 Flickering Prior to AF Termination

The standard deviations of RRI fluctuations for each AF termination sample are significantly different from the values for the AF State (Mann-Whitney test, p-value <0.001 for all). Thus the cardiac state is not AF State prior to termination.

A similar bimodal distribution is observed in 2 of the 20 AF termination samples (dataset no. 7 and 12 in Table 4) (example in Figure 12), where flickering also occurs before AF termination (Figure 13). The boundary value of 0.125 between Near-Normal and Near-AF is also a good approximation in both cases.

For the remainder of the samples, the distributions are dominated by the Near-AF mode (example in Figure 14), where the cardiac state spends most of its time Near-AF (understandably so, since the cardiac rhythm is AF rhythm), while occasionally flickering over to Near-Normal (Figure 15).

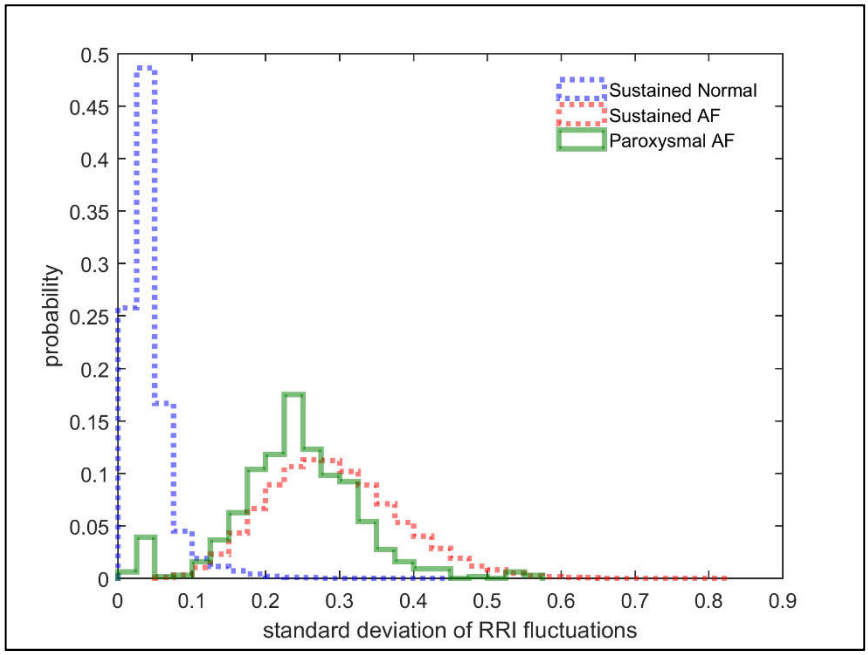

Figure 12. Distribution of standard deviations of RRI fluctuations for an AF termination sample, which is bimodal, superimposed on the distributions for the Normal State and AF State.

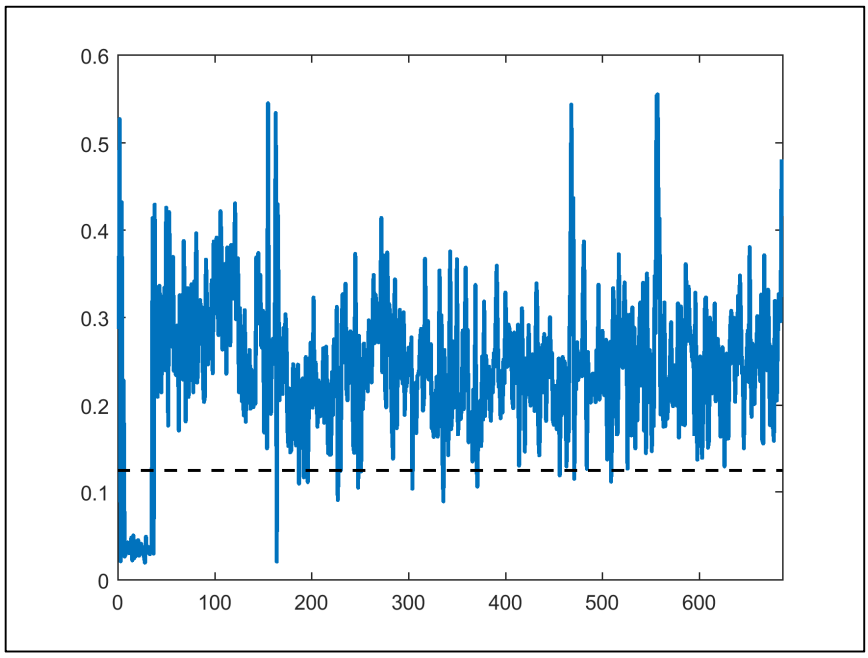

Figure 13. Time series of the standard deviation of RRI fluctuations for the AF termination sample in Figure 12. The horizontal dotted line is the boundary between Near-Normal and Near-AF.

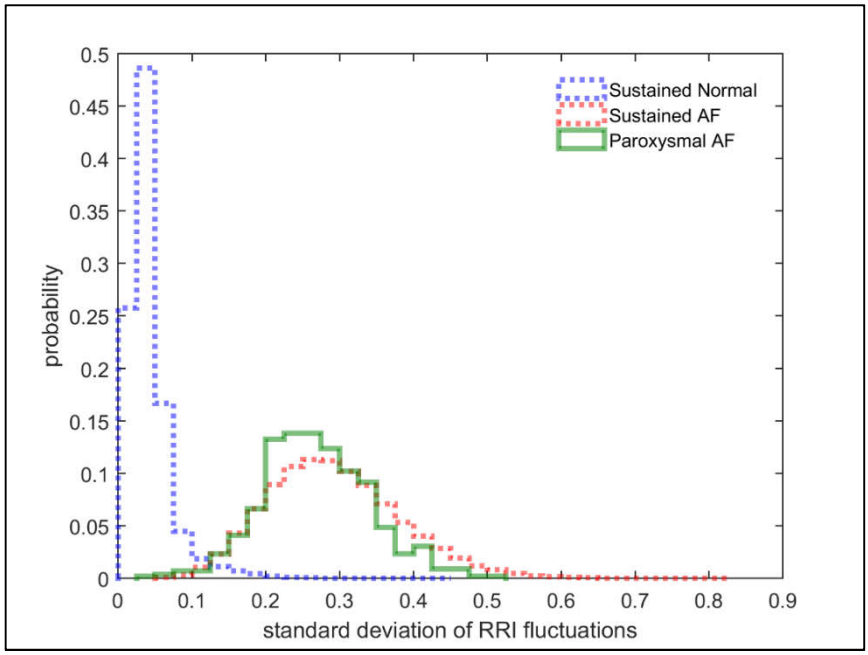

Figure 14. Distribution of standard deviations of RRI fluctuations for an AF termination sample, which is dominated by the Near-AF mode, superimposed on the distributions for the Normal State and AF State.

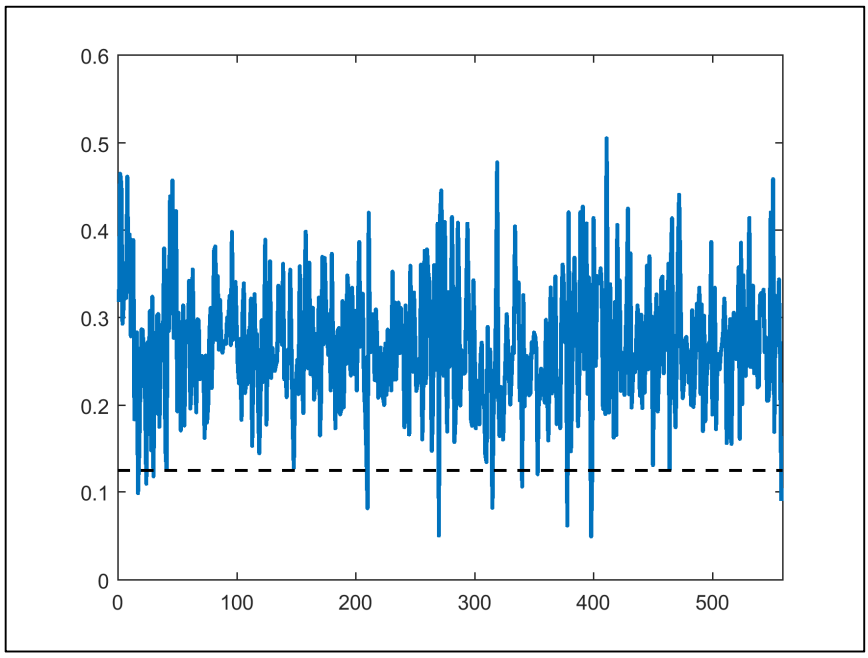

Figure 15. Time series of the standard deviation of RRI fluctuations for the AF termination sample in Figure 14. The horizontal dotted line is the boundary between Near-Normal and Near-AF.

The distribution pattern of the standard deviations of RRI fluctuations, the boundary between Near-Normal and Near-AF, and flickering are robust across all window sizes (for standard deviation calculation) for AF onset as well as termination.

4.2 VT Analysis and Results

4.2.1 Trend in Lag-1 Autocorrelation

Figures 16 and 17 show the lag-1 autocorrelation trends prior to VT onset and termination, respectively.

The lag-1 autocorrelation results prior to VT onset as well as VT termination do not indicate any commonality in trend. Although some samples show an increasing lag-1 autocorrelation close to the critical transition (Figs 16a1, 16a2, 16c1, 16c2 and 16c3), a decreasing trend can be seen in others (Figs 16a4, 16b1, 16b2, 16b4, 17b and 17c), or the lag-1 autocorrelation merely fluctuates without any particular trend (Figs 16a3, 16b3, 16c4 and 17a). This suggests that critical slowing down is not the underlying mechanism for VT onset or termination. The lag-1 autocorrelation results are similar irrespective of the window size of the input data.

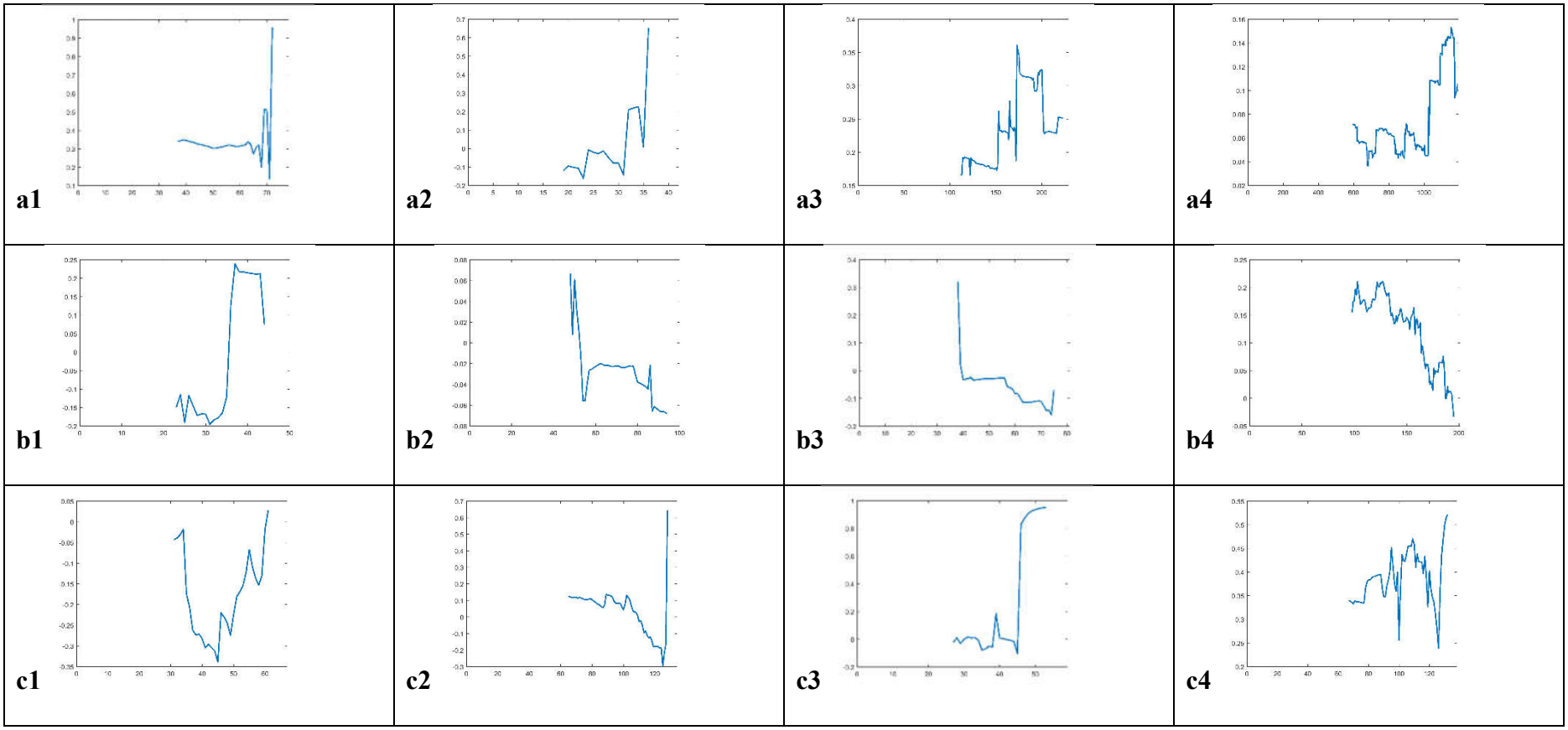

Figure 16. Lag-1 autocorrelation prior to VT onset. Y axis: Autocorrelation at lag-1, X axis: Data index at the end of the moving window used for the autocorrelation calculation. Sequence of samples follow the indexing order in Table 5 (a1=1, a2=2, etc.).

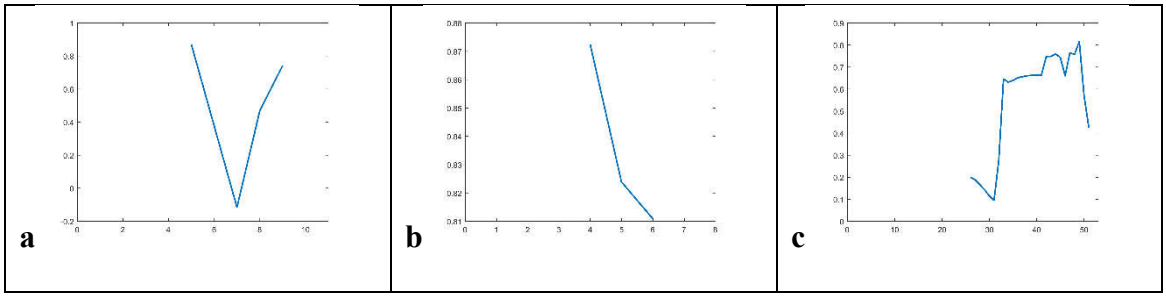

Figure 17. Lag-1 autocorrelation prior to VT termination. Y axis: Autocorrelation at lag-1, X axis: Data index at the end of the moving window used for the autocorrelation calculation. Sequence of samples follow the indexing order in Table 6 (a=1, b=2, c=3).

4.2.2 Flickering Prior to VT Onset

The standard deviations of RRI fluctuations for each Pre-VT sample are significantly different from the values for the Normal State (Mann-Whitney test, p-value <0.001 for all). Thus the cardiac state is not Normal prior to VT onset.

Some of the Pre-VT samples also exhibit bimodality for the distribution of standard deviations of RRI fluctuations (example in Figure 18), where one mode is close to the distribution for the Normal State, and the other mode, which is not close to the distribution for the Normal State, should be close to the VT State. The former and latter modes can thus be characterized as Near-Normal and Near-VT modes respectively. The dividing standard deviation value between these two modes can be approximated by 0.125 also. The cardiac state flickers across this boundary between the two modes (Figure 19).

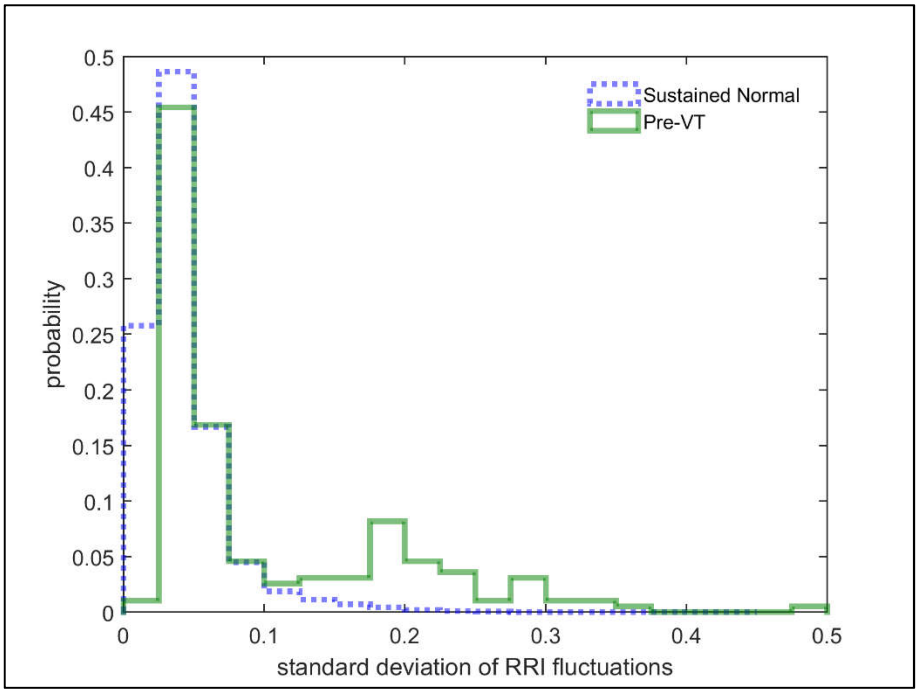

Figure 18. Distribution of standard deviations of RRI fluctuations for a Pre-VT sample, which is bimodal, superimposed on the distribution for the Normal State.

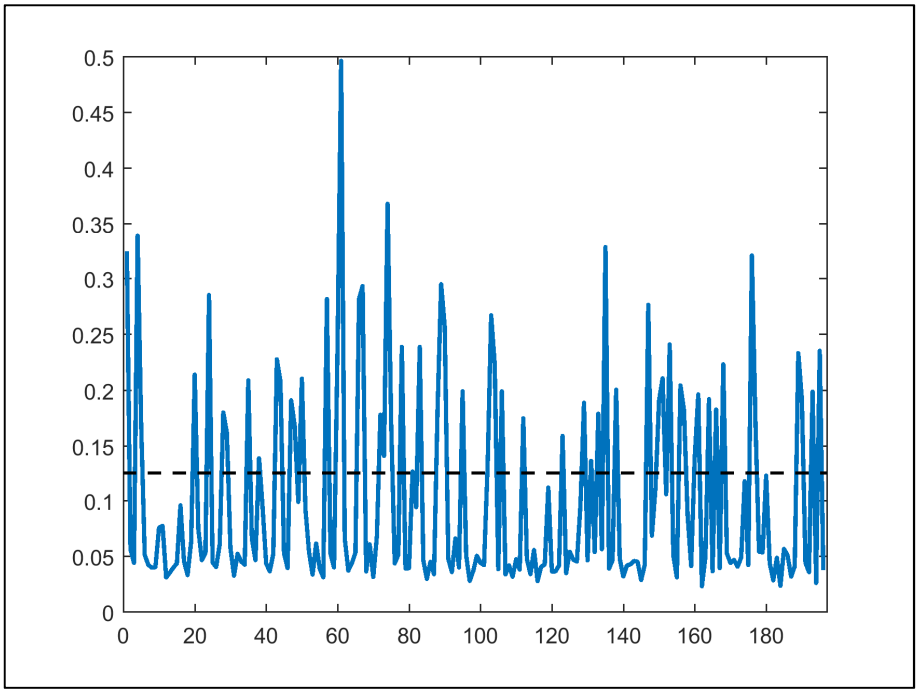

Figure 19. Time series of the standard deviation of RRI fluctuations for the Pre-VT sample in Figure 18. The horizontal dotted line is the boundary between Near-Normal and Near-VT.

A total of 7 out of 12 Pre-VT samples show a bimodal distribution (dataset no. 2, 3, 7-9, 11 and 12 in Table 5), the remaining 5 have a distribution that is dominated by the Near-Normal mode (dataset no. 1, 4-6 and 10 in Table 5) (example in Figure 20), where the cardiac state occasionally flickers to Near-VT (Figure 21).

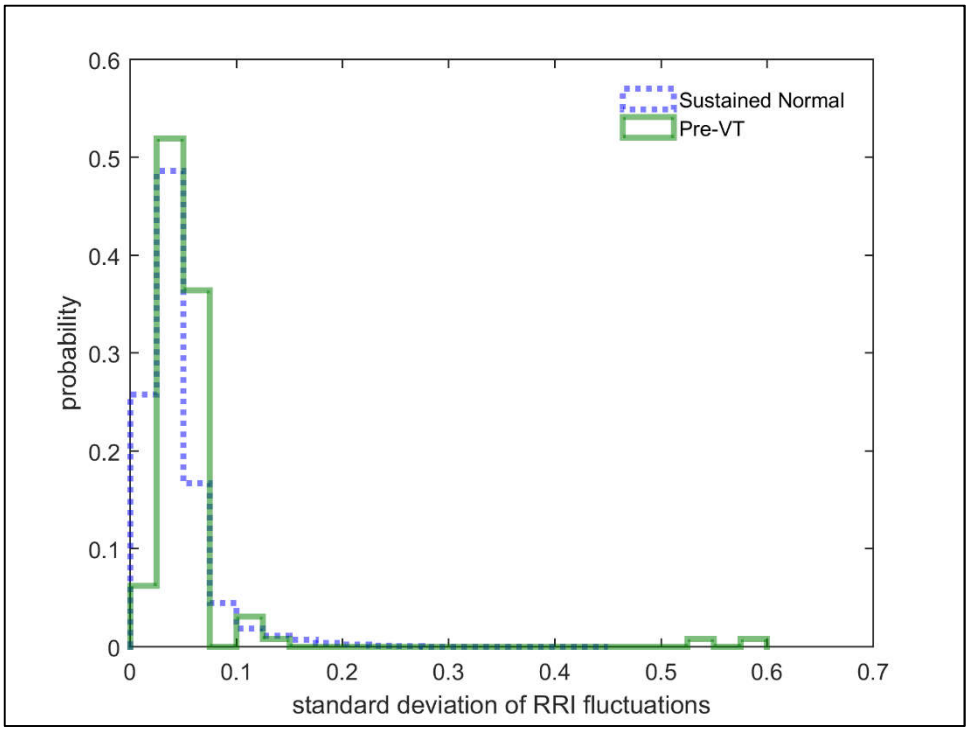

Figure 20. Distribution of standard deviations of RRI fluctuations for a Pre-VT sample, which is dominated by the Near-Normal mode, superimposed on the distribution for the Normal State.

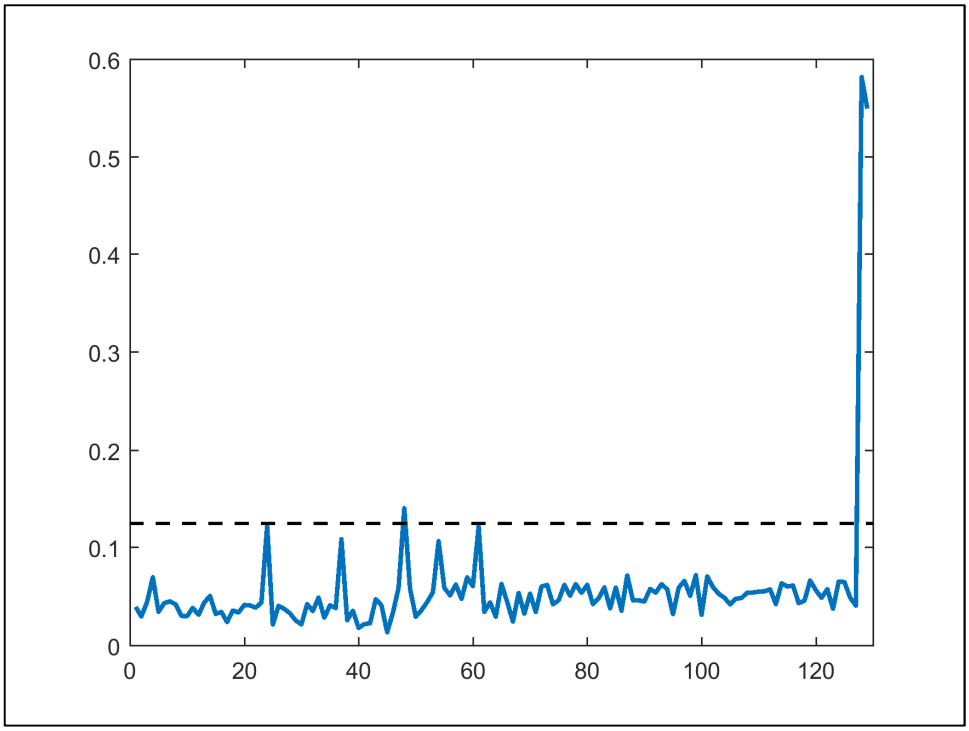

Figure 21. Time series of the standard deviation of RRI fluctuations for the Pre-VT sample in Figure 20. The horizontal dotted line is the boundary between Near-Normal and Near-VT.

4.2.3 Flickering Prior to VT Termination

Within the limited samples available for VT termination, two samples showed a bimodal distribution (dataset no. 1 and 3 in Table 6) (example in Figure 22). The standard-deviation value of 0.125 is a good approximation as well for the boundary between the Near-Normal and Near-VT modes. Prior to VT termination, the cardiac state flickers between Near-Normal and Near-VT (Figure 23). The remaining sample has a distribution that is dominated by the Near-VT mode (Figure 24), where the cardiac state flickers to Near-Normal once (Figure 25).

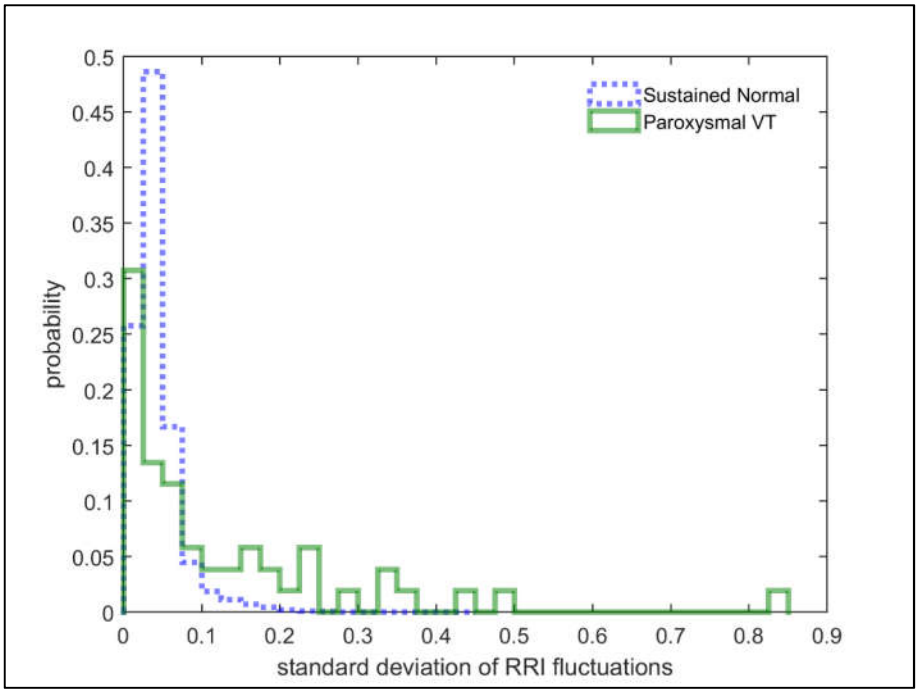

Figure 22. Distribution of standard deviations of RRI fluctuations for a VT termination sample, which is bimodal, superimposed on the distribution for the Normal State.

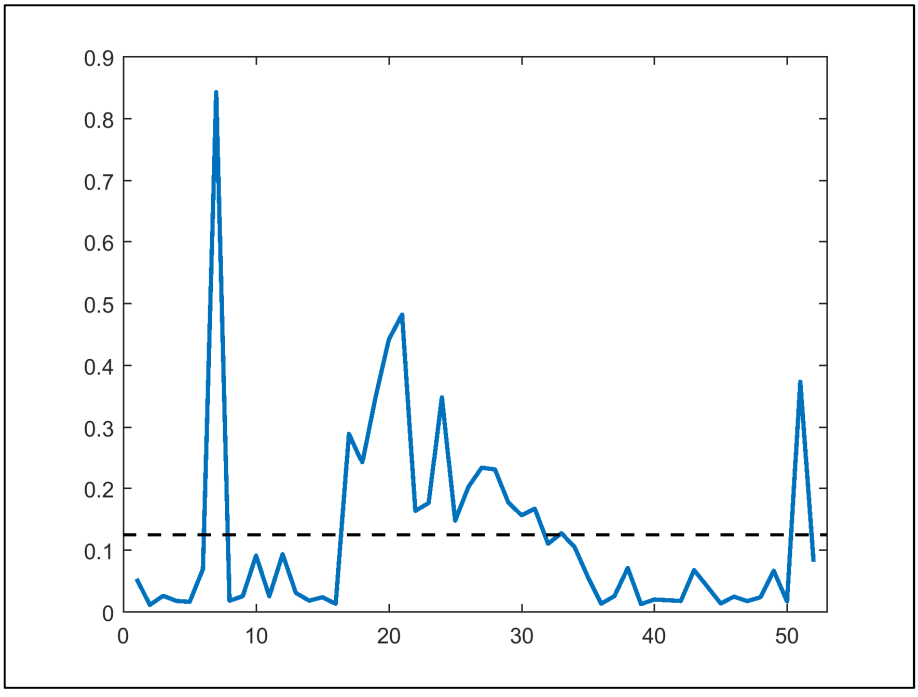

Figure 23. Time series of the standard deviation of RRI fluctuations for the VT termination sample in Figure 22. The horizontal dotted line is the boundary between Near-Normal and Near-VT.

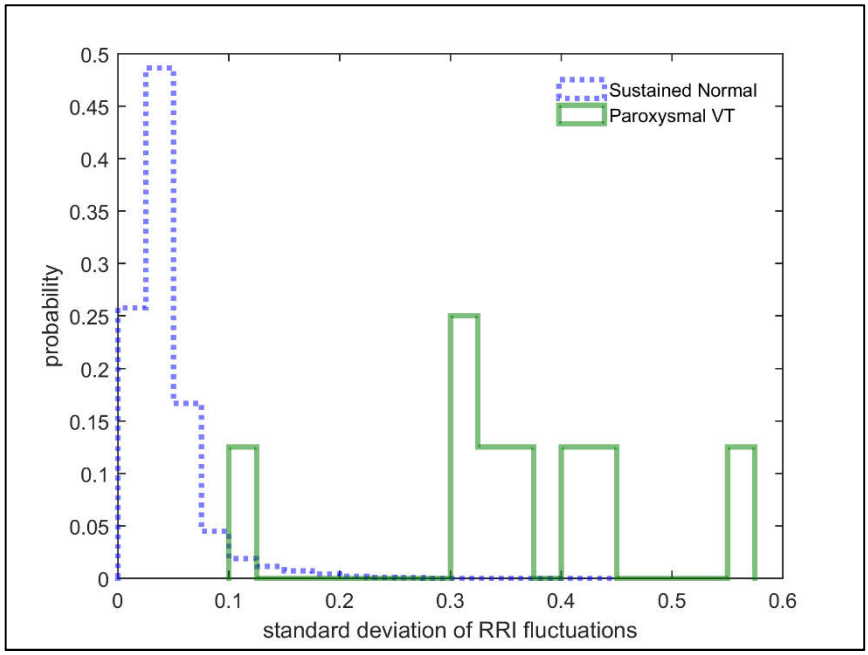

Figure 24. Distribution of standard deviations of RRI fluctuations for a VT termination sample, which is dominated by the Near-VT mode, superimposed on the distribution for the Normal State.

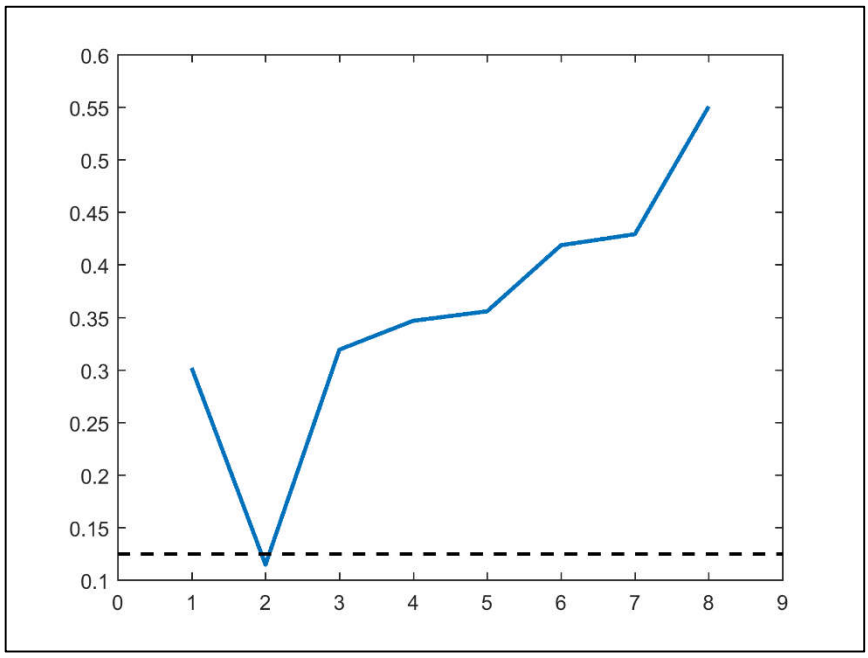

Figure 25. Time series of the standard deviation of RRI fluctuations for the VT termination sample in Figure 24. The horizontal dotted line is the boundary between Near-Normal and Near-VT.

The distribution pattern of the standard deviations of RRI fluctuations, the boundary between Near-Normal and Near-VT, and flickering are robust across all window sizes (for standard deviation calculation) for both VT onset and termination.

CHAPTER 5

SUMMARY AND DISCUSSION

5.1 Summary of Findings

Analysis of the lag-1 autocorrelation of the cardiac state in samples of AF onset as well as termination indicate that critical slowing down is not the mechanism leading to the critical transition. Instead, our results show that the critical transition into and out of paroxysmal AF is preceded by flickering. Supporting evidence of flickering is provided by a bimodal distribution of the cardiac states prior to the critical transition, where the cardiac state flickers between the Near-Normal and Near-AF states attributed to the two modes, respectively.

Similar conclusions can be drawn from our analysis of the VT onset and termination samples; i.e. the critical transition is preceded by flickering, rather than critical slowing down. Similar to AF, the lag-1 autocorrelation of the cardiac state does not always exhibit the increasing trend near the transition as expected for critical slowing down [28]. Evidence of flickering prior to the critical transition into and out of VT is similarly provided by a bimodal distribution of the cardiac states as well as flickering of the cardiac state between the Near-Normal and Near-VT states attributed to the two modes, respectively.

Thus, we conclude that the critical transition for onset and termination of AF and VT is preceded by flickering, contrary to the hypothesis put forward by Olde Rikkert et al. [23]. Clinically, paroxysmal AF has been observed to be triggered by ectopic beats in normal sinus rhythm prior to paroxysmal AF [77-79]. Further analysis of our Pre-AF data also supports this clinical observation. Among the standard deviations of RRI fluctuations that are associated with Near-AF State, those that included at least one or more ectopic beats accounted for 77.29%, 87.10%, 91.51% and 93.51% for window size 5, 10, 15 and 20

respectively, averaged over the 20 Pre-AF datasets. In contrast, among the standard deviations of RRI fluctuations that are associated with Near-Normal State, those that included at least one or more ectopic beats accounted for 8.19%, 8.30%, 6.88% and 8.05% for window size 5, 10, 15 and 20 respectively, averaged over the 20 Pre-AF datasets. In other words, when the cardiac state is near-AF, the beats are dominated by ectopic ones. The ectopic beats are not dominant when the cardiac state is near-Normal.

5.2 Limitations of Study

Although we were unable to obtain data for Incessant VT to serve as reference for the VT State, the Normal State data alone has proven to be sufficient as a reference to construe the Near-VT State. The availability of long term Incessant VT data would enable the boundary separating the standard deviations of RRI fluctuations for Near-Normal and Near-VT to be determined more accurately.

5.3 Potential Applications

The flickering of cardiac state prior to AF or VT onset could be used as an early warning. A simple implementation could involve triggering an alarm if the cardiac state flickers across the boundary between the Near-Normal and Near-Disease states for the first time. It should be pointed out however, that the flickering of cardiac states cannot be employed as the sole indicator, as it is unable to distinguish between the two types of arrhythmia. Other indicators would need to be included in the early warning.

There is increasingly interest in the use of wearable technology with ECG tracking capability to monitor cardiac health, as can be seen in a recently concluded study involving the Apple Watch [80, 81]. The main objective of the Apple Watch study is to determine if measurement of pulse rate irregularity or variability can be used to screen for AF. A small percentage of the participants who volunteered for the initial trial participated in the second phase of the trial, which involved wearing a portable ECG monitor for up to a week [80], if they were notified of a 'potential problem' by the Apple Watch. Approximately 33% of the participants in the second phase were reported to have AF [81]. In this regard, cardiac state flickering could perhaps be used to augment pulse rate irregularity to improve the accuracy of the screening process.

The flickering of cardiac state preceding the onset of AF and VT could be used to guide the development of new pharmaceuticals and control methods to prevent the onset of the arrhythmia. In addition, the flickering of cardiac state preceding the termination of the arrhythmia could be used to guide the development of new termination methods, for example, instead of using random large currents for defibrillation and cardioversion, perhaps using shaped pulses with smaller amplitudes [82-85] and optimised timing might be more effective.

Finally, our methods of defining system states and detection of flickering could potentially be adapted to test the critical slowing down hypothesis for other chronic episodic diseases.

REFERENCES

[1] H. Chu, D. Lee, and K. H. Cho, "Precritical State Transition Dynamics in the Attractor Landscape of a Molecular Interaction Network Underlying Colorectal Tumorigenesis," *PLoS One,* vol. 10, no. 10, p. e0140172, 2015.

[2] J. Ross and A. P. Arkin, "Complex systems: from chemistry to systems biology," *Proc Natl Acad Sci U S A,* vol. 106, no. 16, pp. 6433-4, Apr 21 2009.

[3] E. A. Sobie, "An introduction to dynamical systems," *Sci Signal,* vol. 4, no. 191, p. tr6, Sep 13 2011.

[4] V. Dakos and J. Bascompte, "Critical slowing down as early warning for the onset of collapse in mutualistic communities," *Proceedings of the National Academy of Sciences,* vol. 111, no. 49, pp. 17546-17551, 2014.

[5] M. Hirota, M. Holmgren, E. H. Van Nes, and M. Scheffer, "Global resilience of tropical forest and savanna to critical transitions," *Science,* vol. 334, no. 6053, pp. 232-5, Oct 14 2011.

[6] J. B. Jackson *et al.*, "Historical overfishing and the recent collapse of coastal ecosystems," *Science,* vol. 293, no. 5530, pp. 629-37, Jul 27 2001.

[7] S. Kefi *et al.*, "Spatial vegetation patterns and imminent desertification in Mediterranean arid ecosystems," *Nature,* vol. 449, no. 7159, pp. 213-7, Sep 13 2007.

[8] P. J. Mumby, A. Hastings, and H. J. Edwards, "Thresholds and the resilience of Caribbean coral reefs," *Nature,* vol. 450, no. 7166, pp. 98-101, Nov 1 2007.

[9] M. Scheffer, S. Carpenter, J. A. Foley, C. Folke, and B. Walker, "Catastrophic shifts in ecosystems," *Nature,* vol. 413, no. 6856, pp. 591-6, Oct 11 2001.

[10] T. M. Lenton *et al.*, "Tipping elements in the Earth's climate system," *Proc Natl Acad Sci U S A,* vol. 105, no. 6, pp. 1786-93, Feb 12 2008.

[11] S. Drijfhout *et al.*, "Catalogue of abrupt shifts in Intergovernmental Panel on Climate Change climate models," *Proceedings of the National Academy of Sciences,* vol. 112, no. 43, pp. E5777-E5786, 2015.

[12] J. Bakke *et al.*, "Rapid oceanic and atmospheric changes during the Younger Dryas cold period," *Nature Geoscience,* vol. 2, p. 202, 02/15/online 2009.

[13] R. M. May, S. A. Levin, and G. Sugihara, "Complex systems: ecology for bankers," *Nature,* vol. 451, no. 7181, pp. 893-5, Feb 21 2008.

[14] A. G. Haldane and R. M. May, "Systemic risk in banking ecosystems," *Nature,* vol. 469, no. 7330, pp. 351-5, Jan 20 2011.

[15] J. G. Venegas *et al.*, "Self-organized patchiness in asthma as a prelude to catastrophic shifts," *Nature,* vol. 434, no. 7034, pp. 777-82, Apr 7 2005.

[16] I. A. van de Leemput *et al.*, "Critical slowing down as early warning for the onset and termination of depression," *Proc Natl Acad Sci U S A,* vol. 111, no. 1, pp. 87-92, Jan 7 2014.

[17] T. Zeng, C. C. Zhang, W. Zhang, R. Liu, J. Liu, and L. Chen, "Deciphering early development of complex diseases by progressive module network," *Methods,* vol. 67, no. 3, pp. 334-43, Jun 1 2014.

[18] M. Li, T. Zeng, R. Liu, and L. Chen, "Detecting tissue-specific early warning signals for complex diseases based on dynamical network biomarkers: study of type 2 diabetes by cross-tissue analysis," *Brief Bioinform,* vol. 15, no. 2, pp. 229-43, Mar 2014.

[19] B. Litt *et al.*, "Epileptic seizures may begin hours in advance of clinical onset: a report of five patients," *Neuron,* vol. 30, no. 1, pp. 51-64, Apr 2001.

[20] M. A. Kramer *et al.*, "Human seizures self-terminate across spatial scales via a critical transition," *Proc Natl Acad Sci U S A,* vol. 109, no. 51, pp. 21116-21, Dec 18 2012.

[21] P. E. McSharry, L. A. Smith, and L. Tarassenko, "Prediction of epileptic seizures: are nonlinear methods relevant?," *Nat Med,* vol. 9, no. 3, pp. 241-2; author reply 242, Mar 2003.

[22] C. Trefois, P. M. Antony, J. Goncalves, A. Skupin, and R. Balling, "Critical transitions in chronic disease: transferring concepts from ecology to systems medicine," *Curr Opin Biotechnol,* vol. 34, pp. 48-55, Aug 2015.

[23] M. G. Olde Rikkert *et al.*, "Slowing Down of Recovery as Generic Risk Marker for Acute Severity Transitions in Chronic Diseases," (in eng), *Crit Care Med,* vol. 44, no. 3, pp. 601-6, Mar 2016.

[24] J. C. Foo *et al.*, "Dynamical state transitions into addictive behaviour and their early-warning signals," *Proc Biol Sci,* vol. 284, no. 1860, Aug 16 2017.

[25] L. Lahti, J. Salojarvi, A. Salonen, M. Scheffer, and W. M. de Vos, "Tipping elements in the human intestinal ecosystem," *Nat Commun,* vol. 5, p. 4344, 2014.

[26] Y. Kuznetsov, *Elements of applied bifurcation theory* (Applied mathematical sciences, no. 112). New York: Springer-Verlag, 1995, pp. xv, 515 p.

[27] M. Scheffer *et al.*, "Early-warning signals for critical transitions," (in eng), *Nature,* vol. 461, no. 7260, pp. 53-9, Sep 03 2009.

[28] M. Scheffer *et al.*, "Anticipating critical transitions," (in eng), *Science,* vol. 338, no. 6105, pp. 344-8, Oct 19 2012.

[29] C. Wissel, "A universal law of the characteristic return time near thresholds," *Oecologia,* vol. 65, no. 1, pp. 101-107, Dec 1984.

[30] E. H. van Nes and M. Scheffer, "Slow recovery from perturbations as a generic indicator of a nearby catastrophic shift," *Am Nat,* vol. 169, no. 6, pp. 738-47, Jun 2007.

[31] A. J. Veraart, E. J. Faassen, V. Dakos, E. H. van Nes, M. Lurling, and M. Scheffer, "Recovery rates reflect distance to a tipping point in a living system," *Nature,* vol. 481, no. 7381, pp. 357-9, Dec 25 2011.

[32] V. Dakos, M. Scheffer, E. H. van Nes, V. Brovkin, V. Petoukhov, and H. Held, "Slowing down as an early warning signal for abrupt climate change," *Proc Natl Acad Sci U S A,* vol. 105, no. 38, pp. 14308-12, Sep 23 2008.

[33] W. Horsthemke and R. Lefever, *Noise-Induced Transitions: Theory and Applications in Physics, Chemistry, and Biology*. Springer, 1984.

[34] R. Wang *et al.*, "Flickering gives early warning signals of a critical transition to a eutrophic lake state," *Nature,* vol. 492, no. 7429, pp. 419-22, Dec 20 2012.

[35] M. Scheffer and Harry E. Humphreys Book Fund., *Critical transitions in nature and society* (Princeton studies in complexity). Princeton, N.J.: Princeton University Press, 2009, pp. xi, 384 p.

[36] V. Dakos *et al.*, "Methods for detecting early warnings of critical transitions in time series illustrated using simulated ecological data," *PLoS One,* vol. 7, no. 7, p. e41010, 2012.

[37] S. R. Carpenter and W. A. Brock, "Rising variance: a leading indicator of ecological transition," *Ecol Lett,* vol. 9, no. 3, pp. 311-8, Mar 2006.

[38] S. R. Carpenter, W. A. Brock, J. J. Cole, J. F. Kitchell, and M. L. Pace, "Leading indicators of trophic cascades," *Ecol Lett,* vol. 11, no. 2, pp. 128-38, Feb 2008.

[39] P. U. Clark, N. G. Pisias, T. F. Stocker, and A. J. Weaver, "The role of the thermohaline circulation in abrupt climate change," *Nature,* vol. 415, no. 6874, pp. 863-9, Feb 21 2002.

[40] W. C. Chang *et al.*, "Loss of neuronal network resilience precedes seizures and determines the ictogenic nature of interictal synaptic perturbations," *Nat Neurosci,* vol. 21, no. 12, pp. 1742-1752, Dec 2018.

[41] L. Glass, "Dynamical disease: Challenges for nonlinear dynamics and medicine," *Chaos,* vol. 25, no. 9, p. 097603, Sep 2015.

[42] J. N. Weiss, M. Nivala, A. Garfinkel, and Z. Qu, "Alternans and arrhythmias: from cell to heart," *Circ Res,* vol. 108, no. 1, pp. 98-112, Jan 7 2011.

[43] M. C. Mackey and J. G. Milton, "Dynamical diseases," *Ann N Y Acad Sci,* vol. 504, pp. 16-32, 1987.

[44] L. Glass and M. C. Mackey, "Pathological conditions resulting from instabilities in physiological control systems," *Ann N Y Acad Sci,* vol. 316, pp. 214-35, 1979.

[45] M. C. Mackey and L. Glass, "Oscillation and chaos in physiological control systems," *Science,* vol. 197, no. 4300, pp. 287-9, Jul 15 1977.

[46] A. Garfinkel *et al.*, "Quasiperiodicity and chaos in cardiac fibrillation," *J Clin Invest,* vol. 99, no. 2, pp. 305-14, Jan 15 1997.

[47] J. N. Weiss, A. Garfinkel, H. S. Karagueuzian, Z. Qu, and P. S. Chen, "Chaos and the transition to ventricular fibrillation: a new approach to antiarrhythmic drug evaluation," (in eng), *Circulation,* vol. 99, no. 21, pp. 2819-26, Jun 1 1999.

[48] H. S. Karagueuzian, H. Stepanyan, and W. J. Mandel, "Bifurcation theory and cardiac arrhythmias," *Am J Cardiovasc Dis,* vol. 3, no. 1, pp. 1-16, 2013.

[49] M. Small, D. Yu, and R. G. Harrison, "Observation of a period doubling bifurcation during onset of human ventricular fibrillation," *International Journal of Bifurcation and Chaos,* vol. 13, no. 3, pp. 743–754, 2002.

[50] F. Shaffer and J. P. Ginsberg, "An Overview of Heart Rate Variability Metrics and Norms," *Front Public Health,* vol. 5, p. 258, 2017.

[51] Task Force of the European Society of Cardiology and the North American Society of Pacing and Electrophysiology, "Heart rate variability: standards of measurement, physiological interpretation and clinical use. ," *Circulation,* vol. 93, no. 5, pp. 1043-65, Mar 1 1996.

[52] F. Shaffer, R. McCraty, and C. L. Zerr, "A healthy heart is not a metronome: an integrative review of the heart's anatomy and heart rate variability," *Front Psychol,* vol. 5, p. 1040, 2014.

[53] American Heart Association. *About Arrhythmia*. Available: http://www.heart.org/HEARTORG/Conditions/Arrhythmia/AboutArrhythmia/About-Arrhythmia_UCM_002010_Article.jsp

[54] American Heart Association. (2015, Nov 23, 2015). *All About Heart Rate (Pulse)*. Available: http://www.heart.org/HEARTORG/Conditions/More/MyHeartandStrokeNews/All-About-Heart-Rate-Pulse_UCM_438850_Article.jsp#.VlKNkHYrK9I

[55] R. Simpson, J. Langtree, and A. Mitchell, "Ectopic beats: How many count?," *EMJ Cardiol.,* vol. 5, no. 1, pp. 88-92, 2017.

[56] American Heart Association. *Premature Contractions - PACs and PVCs*. Available: http://www.heart.org/HEARTORG/Conditions/Arrhythmia/AboutArrhythmia/Premature-Contractions---PACs-and-PVCs_UCM_302043_Article.jsp

[57] NHLBI. *Arrhythmia*. Available: www.nhlbi.nih.gov/health-topics/arrhythmia

[58] V. Markides and R. J. Schilling, "Atrial fibrillation: classification, pathophysiology, mechanisms and drug treatment," *Heart,* vol. 89, no. 8, pp. 939-43, Aug 2003.

[59] MayoClinic. *Ventricular tachycardia*. Available: https://www.mayoclinic.org/diseases-conditions/ventricular-tachycardia/symptoms-causes/syc-20355138

[60] Healio. *Ventricular Tachycardia (VT) ECG Review*. Available: https://www.healio.com/cardiology/learn-the-heart/ecg-review/ecg-topic-reviews-and-criteria/ventricular-tachycardia-review

[61] C. J. MacIntyre and J. L. Sapp, "Treatment of persistent ventricular tachycardia: Drugs or ablation?," *Trends Cardiovasc Med,* vol. 27, no. 7, pp. 506-513, Oct 2017.

[62] J. Shenthar, "Unusual Incessant Ventricular Tachycardia: What Is the Underlying Cause and the Possible Mechanism?," *Circ Arrhythm Electrophysiol,* vol. 8, no. 6, pp. 1507-11, Dec 2015.

[63] B. L. Lan and M. Toda, "Fluctuations of healthy and unhealthy heartbeat intervals," *EPL (Europhysics Letters),* vol. 102, pp. 18002, p1-p6, 2013.

[64] A. Chakraborti, I. M. Toke, M. Patriarca, and F. Abergel, "Econophysics review: I. Empirical facts," *Quantitative Finance,* vol. 11, no. 7, pp. 991-1012, 2011/07/01 2011.

[65] The MIT-BIH Normal Sinus Rhythm Database. Available: https://www.physionet.org/physiobank/database/nsrdb/

[66] The Long-Term AF Database. Available: https://www.physionet.org/physiobank/database/ltafdb/

[67] S. Petrutiu, A. V. Sahakian, and S. Swiryn, "Abrupt changes in fibrillatory wave characteristics at the termination of paroxysmal atrial fibrillation in humans," *Europace,* vol. 9, no. 7, pp. 466-70, Jul 2007.

[68] J. B. Shea and S. F. Sears, "A Patient's Guide to Living With Atrial Fibrillation," *Circulation,* vol. 117, no. 20, pp. e340-e343, 2008.

[69] A. L. Goldberger *et al.*, "PhysioBank, PhysioToolkit, and PhysioNet: components of a new research resource for complex physiologic signals," *Circulation,* vol. 101, no. 23, pp. E215-20, Jun 13 2000.

[70] PhysioNet. Available: https://physionet.org/

[71] G. B. Moody and R. G. Mark, "The impact of the MIT-BIH arrhythmia database," *IEEE Eng Med Biol Mag,* vol. 20, no. 3, pp. 45-50, May-Jun 2001.

[72] MIT-BIH Arrhythmia Database. Available: https://www.physionet.org/physiobank/database/mitdb/

[73] Harvard-MIT Division of Health Sciences and Technology. *MIT-BIH Arrhythmia Database Directory*. Available: https://www.physionet.org/physiobank/database/html/mitdbdir/mitdbdir.htm

[74] The MIT-BIH Malignant Ventricular Arrhythmia Database. Available: https://physionet.org/physiobank/database/vfdb/

[75] S. D. Greenwald, "Development and analysis of a ventricular fibrillation detector.," M.S. thesis, Dept. of Electrical Engineering and Computer Science, MIT, 1986.

[76] G. E. P. Box, G. M. Jenkins, and G. C. Geinsel, *Time Series Analysis Forecasting and Control*. New Jersey: Wiley, 2008.

[77] T. Killip and J. H. Gault, "Mode of Onset of Atrial Fibrillation in Man," *Am Heart J,* vol. 70, pp. 172-9, Aug 1965.

[78] J. E. Waktare *et al.*, "The role of atrial ectopics in initiating paroxysmal atrial fibrillation," *Eur Heart J,* vol. 22, no. 4, pp. 333-9, Feb 2001.

[79] M. Haissaguerre *et al.*, "Spontaneous initiation of atrial fibrillation by ectopic beats originating in the pulmonary veins," *N Engl J Med,* vol. 339, no. 10, pp. 659-66, Sep 3 1998.

[80] M. P. Turakhia *et al.*, "Rationale and design of a large-scale, app-based study to identify cardiac arrhythmias using a smartwatch: The Apple Heart Study," *Am Heart J,* vol. 207, pp. 66-75, Jan 2019.

[81] Stanford School of Medicine. *Apple Heart Study*. Available: http://med.stanford.edu/appleheartstudy.html

[82] N. A. Trayanova and L. J. Rantner, "New insights into defibrillation of the heart from realistic simulation studies," *EP Europace,* vol. 16, no. 5, pp. 705–713, 2014.

[83] W. Li, A. H. Janardhan, V. V. Fedorov, Q. Sha, R. B. Schuessler, and I. R. Efimov, "Low-energy multistage atrial defibrillation therapy terminates atrial fibrillation with less energy than a single shock," *Circ Arrhythm Electrophysiol,* vol. 4, no. 6, pp. 917-25, Dec 2011.

[84] S. Luther *et al.*, "Low-energy control of electrical turbulence in the heart," *Nature,* vol. 475, no. 7355, pp. 235-9, Jul 13 2011.

[85] P. Walsh *et al.*, "Towards Low Energy Atrial Defibrillation," *Sensors (Basel),* vol. 15, no. 9, pp. 22378-400, Sep 3 2015.